ADVANCED HEALTHCARE MATERIALS
www.advhealthmat.de

Computational Fluid Dynamics (CFD) Analysis of Bioprinting

*Umar Naseef Mohamed Fareez, Syed Ali Arsal Naqvi, Makame Mahmud, and Mikail Temirel**

Regenerative medicine has evolved with the rise of tissue engineering due to advancements in healthcare and technology. In recent years, bioprinting has been an upcoming approach to traditional tissue engineering practices, through the fabrication of functional tissue by its layer-by-layer deposition process. This overcomes challenges such as irregular cell distribution and limited cell density, and it can potentially address organ shortages, increasing transplant options. Bioprinting fully functional organs is a long stretch but the advancement is rapidly growing due to its precision and compatibility with complex geometries. Computational Fluid Dynamics (CFD), a carestone of computer-aided engineering, has been instrumental in assisting bioprinting research and development by cutting costs and saving time. CFD optimizes bioprinting by testing parameters such as shear stress, diffusivity, and cell viability, reducing repetitive experiments and aiding in material selection and bioprinter nozzle design. This review discusses the current application of CFD in bioprinting and its potential to enhance the technology that can contribute to the evolution of regenerative medicine.

1. Introduction

As the world is fast-forwarding in terms of technology, the future of healthcare is advancing too, giving researchers more options to integrate it in the medical fields. The latest developments in the field of nanotechnology and 3D printing gave doctors an opportunity to find effective alternative cures. Within the scope of additive manufacturing (AM), apart from the achievements of 3D printing to print prostheses and design implants,[1] bioprinting has given possible ways to successfully grow tissues and further organs, a step forward in tissue engineering.[2] This is a major progress in terms of helping patients receive a functional tissue or organ after losing an organ or damaging tissues after an injury or because of genetic abnormalities.

Tissue engineering is an interdisciplinary field that focuses on how new biological functional substitutes can be developed to serve the purpose of regenerating damaged tissues from living cells.[3] W. T. Green, M.D., a pediatric orthopedic surgeon conducted experiments to generate cartilage in the early 1970s, failed to regenerate cartilage tissue, yet assured a promising advanced future of tissue engineering with the upcoming biocompatible materials that will be developed later in the years.[4] This revolutionary concept was first introduced in the early 1970s and further applied in various areas of specialization, resulting in extensive research in skin tissues, heart tissues, and cartilage tissues. The significance of tissue engineering is that it gives the potential that damaged tissues can be replaced with new ones through bioengineering in a laboratory environment and then later implanted within the human body.[5]

Tissue engineering, with the help of AM techniques, has shown more favorable solutions to complications found during the traditional tissue engineering process. Traditional tissue engineering techniques include adding regenerative cells to a scaffold containing growth factors and eventually allowing a functional matrix to be formed. The main factor that brings this technique to a disadvantage is that the required result is not often achieved due to the irregular distribution of cells within the mixture. However, the utilization of 3D bioprinting that prints on a layer-by-layer basis thus further allows to obtain the desired complex geometries and generate functional tissues.[6] As mentioned earlier, the shortage of donated healthy organs has created a demand for bioprinting technologies due to their favorable approaches in terms of generating highly precise tissues that are not rejected by the host body's immune system, thus raising the possibility of lab-grown organ transplantation.[2] Moreover, a few other notable characteristics of bioprinting include its ability to "adaptability to a traditional, modular or mixed approach" and capacity to print details down to the range of 50–200 μm.[5] Conventional bioprinting techniques usually follow a layer-by-layer manner to construct 3D structures, like extrusion-based, droplet-based, and laser-assisted including digital light processing (DLP) and stereolithography (SLA).[7] There are also some new technologies that

U. N. M. Fareez, S. A. A. Naqvi, M. Mahmud, M. Temirel
Mechanical Engineering Department, School of Engineering
Abdullah Gul University
Kayseri 38080, Turkey
E-mail: mikail.temirel@agu.edu.tr

The ORCID identification number(s) for the author(s) of this article can be found under https://doi.org/10.1002/adhm.202400643

DOI: 10.1002/adhm.202400643

do not follow the layer-by-layer method such as volumetric bioprinting (VBP), which is a notable advancement in bioprinting, also known as computed axial lithography (CAL), that enables printing large cm-scaled structures in a considerable short time with high resolution.[8] In addition to that, with the increasing research in the field of bioprinting, the application of computational methods has increased significantly to ensure the most accurate results.

Computational fluid dynamics or in short CFD is a branch of fluid dynamics that has been applied in various engineering fields that uses a combination of both numerical analysis and computational software to solve complex fluid-related problems.[9] CFD modeling and its importance can be seen in the field of aerospace, where the most accurate fluid flow is analyzed with varying boundary conditions that help the engineers detect and fix possible design errors during the initial phase.[10] This is one of the various places CFD is constantly used in R&D sectors of such industries. The importance of CFD is not limited to only the aerospace or automotive industries; rather, it is applicable in the field of bioengineering, with more researchers' growing interest toward its practical use. Moreover, CFD is more popular as a cost-saving alternative with very accurate results compared to experimental results.[11]

Within the scope of bioprinting, CFD has been an important tool for testing specified printing parameters such as nozzle speed, shear stress, printability, cell viability, and so on. Testing these parameters with multiple repetitions increases the cost and the time it takes to obtain accurate results. CFD decreases the number of repetitions thus making it more efficient for research.[12] For instance, the bioink used for the experiments conducted for analysis of printability is costly. Using CFD, the flow behaviors and deformation of the material under stresses can be computationally studied. In one study, OpenFOAM software was utilized to study the relation between hydrogel mass flow rate, different nozzle designs, and operating pressure.[13] Similarly, other CFD softwares such as ANSYS Fluent, COMSOL, and FLOW-3D have been used to study further design parameters and nozzle designs. CFD for bioprinting is not limited to nozzle designs but goes beyond to simulate the relation between the characteristics of bioink and nozzle designs on cell viability. In another study, COMSOL was used to compare the effect of shear stress on cell viability between cylindrical and conical nozzles.[14]

This review paper provides an overview of CFD applications in bioprinting technology with the most recent studies in the literature. The study may pave the way toward improving the performance of bioprinting with the help of CFD.

2. Bioprinting Methods and Materials

2.1. Bioprinting

Traditional tissue engineering strategies involved the seeding of cells onto scaffolds, which are solid structures that maintain the shape and mechanical properties of the tissue and provide a substrate for cell attachment and proliferation.[15] However, the limitations of traditional strategies such as limited cell density, lower precision in cell placements, the inability to control pore distribution, and difficulties in manufacturing patient-specific tissues required new techniques to solve prevalent challenges.[16] Bioprinting was initially developed in the 1980s to construct 2D tissues, but only recently has the technology become capable of constructing 3D constructs. However, even with current advancements in scaffold manufacturing technologies, there is a long way to go to fully develop and substitute human organs with bioprinting.[17]

Bioprinting is a game changer in the rapid manufacturing of tissue constructs and provides great benefits that solve some of the problems related to traditional tissue engineering techniques.[18] Bioprinting can be defined as the spatial arrangement of living cells, biomaterials, and biologics in a layer-by-layer fashion to obtain a 3D structure that mimics tissue constructs and can be used for regenerative medicine, cancer research, and tissue engineering.[18] 3D printing completely functional organs is a long-term goal; nonetheless, the field is moving in the correct direction, and research is being conducted to close the gap between reality and imagination.[17]

Typical stages for bioprinting a tissue construct from start to finish involve pre-processing, processing, and post-processing steps.[19] Pre-processing involves target-specific cell culturing and generating a 3D scaffold model of the tissue construct. First, specific cells are isolated and proliferated to large numbers to be used later in the processing stage. Second, MRI or CT scan images of the targeted tissue are generated which are processed and reconstructed to a 3D image format. G-code, which is the pathway that a bioprinter nozzle would follow in a spatial arrangement, is extracted from the 3D image format, and sent to the 3D bioprinter for the processing stage.[20] In the processing stage, isolated and cultured cells from the pre-processing are mixed with hydrogel and biologics to form the bioink for the scaffold-based fabrication. Scaffold-based fabrication consists of three major strategies: droplet, laser, and extrusion-based. In most of these strategies, the G-code dictates the movement of the extruder, and 3D cell-laden constructs are produced. Post-processing might involve a bioreactor or crosslinking mechanisms that would provide a mechanical or chemical stimulus to reinforce the development and maturation of tissue constructs until they reach their desired application.[20]

2.2. Types of Bioprinting Modalities

There are two main categories for bioprinting modalities, scaffold-based and scaffold-free. Scaffold-based bioprinting is further divided into three major fabrication techniques, namely: extrusion-based, droplet-based, and laser-based.[21] The emergence of fused deposition modeling paved the way for the 3D printing of intricate geometries which was later introduced into tissue engineering to create porous scaffolds that act as a solid structure for cell attachment, proliferation, and cell growth.[22]

2.2.1. Scaffold-Based Bioprinting

Extrusion-Based Bioprinting: In extrusion-based bioprinting, the bioink is released via an extruder, which is controlled via an automated three-axis robotic system, in a precise deposition of cells in cylindrical filaments.[21] These cylindrical filaments form the desired 3D porous scaffolds layer by layer. The robotic system is guided by the G-code from computer-aided design

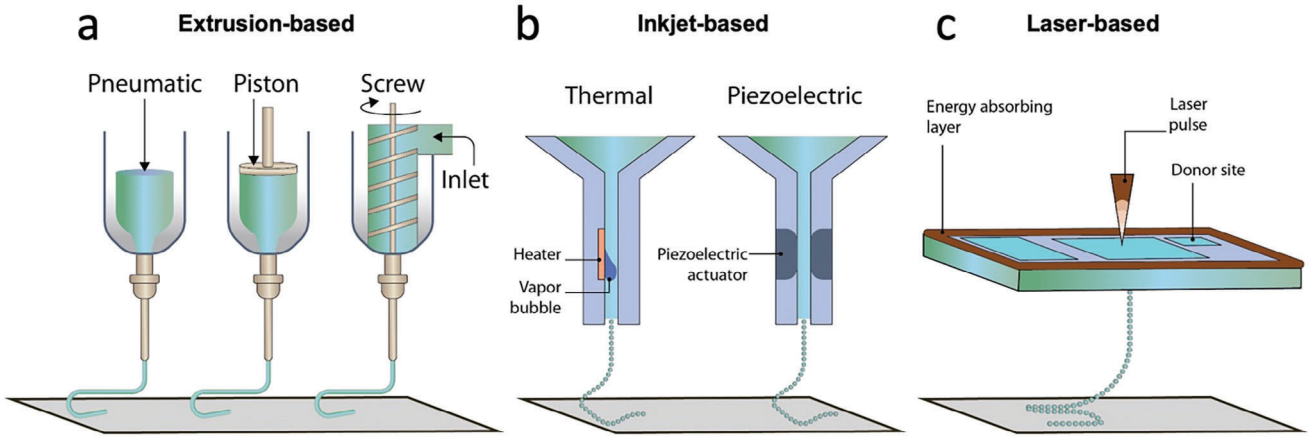

Figure 1. Selected 3D bioprinting approaches. a) Extrusion-based bioprinting method involving three types: pneumatic, piston-driven, and screw-driven dispensing systems to deposit a continuous filament of bioink-containing cells. b) Two components of inkjet bioprinting, thermal and piezoelectric activated printing. Thermal print head is heated electrically to produce air-pressure pulses that force the droplet from the nozzle, whereas a mechanical pulse produced by an actuator to force the materiel as a droplet in piezoelectric-activated printing head. c) Laser-assisted bioprinters. The laser focuses its energy on an absorptive layer, generating a vapor bubble within bioink-containing cells. This process facilitates the transfer of bioink droplets encapsulating cells onto a substrate.

(CAD) software, which enables the user to print rapidly by loading the CAD file. The CAD file is obtained from the scanned images by MRI or CT as highlighted above in the pre-processing stage.[23] Some extrusion-based printer also consists of a fiber optic light source for disposition area activation, a photo initiator, piezoelectric humidifier for crosslinking the materiel right after deposition, and a video camera for x–y–z axis control.[24] For minimum retooling, some printers consist of multiple heads to decrease the print time or to deposit multiple materials.[25] Extrusion-based bioprinting is further divided into two main mechanisms (**Figure 1a**), namely: pneumatic and mechanical. A pneumatic-based system utilizes air pressure to push the bioink out of the nozzle by using a valve-based or valve-free configuration.[26] A mechanical system involves a mechanical device such as a piston or screw to extrude the bioink from the nozzle, and both have their respective pros and cons.[27] The flexibility of materials such as biocompatible copolymers, cell spheroids, and hydrogels that can be used and deposited in the form of continuous beads adds to their functionality.

Droplet-Based Bioprinting: Droplet-based bioprinting involves manipulating the bioink via gravity, atmospheric pressure, and fluid mechanics such that the nozzle ejects a controlled volume of bioink in a droplet fashion.[22] A controlled volume of bioink deposition at predefined locations offers great control, agility, versatility, and simplicity as opposed to extrusion and laser-based bioprinting.[24] Droplet-based bioprinting can be further divided into inkjet, acoustic, and micro-valve bioprinting modules, which have their pros and cons over each other.[28] Acoustic method utilizes the acoustic field to eject droplets, while the micro-valve uses a pressurized reservoir and a nozzle which is electromechanically controlled to create droplets. Inkjet modality further divides into continuous, thermal, piezoelectric, electrostatic, and electrohydrodynamic jet bioprinting, all of which are operated via different mechanisms.[21,22] The most favored Inkjet based bioprinting methods are the ones with thermal and piezoelectric printing heads (Figure 1b). In thermal inkjet printers, the print head is heated electronically, which allows pulses of pressure to eject drops from the heated nozzle, which can heat up from 200 to 300 °C under localized heating without affecting the stability of the biological substances.[24,29] Furthermore, some inkjet printers also contain a piezoelectric crystal that splits the liquid into droplets at regular intervals using an acoustic wave inside the nozzle. This occurs when a voltage is applied to the crystal; it changes its shape rapidly, generating the pressure required to eject droplets.[30]

Laser-Based Bioprinting: Laser-based or laser-assisted bioprinting uses LIFT (laser-induced forward transfer) technology for high-resolution patterning. The setup consists of three major parts (Figure 1c): a laser pulse source, a receiving substrate, and a ribbon.[31] Lasers with a wavelength of ultraviolet in the electromagnetic spectrum or near ultraviolet are used as energy pulses directed toward the ribbon. The ribbon comprises three layers: transparent glass, a laser-absorbing metal, and a layer. The energy pulses directed toward the ribbon melt the metal layer which creates a pressure vacuum for the bioink to form a bubble that drops onto the receiving substrate. This method can continuously print individual cells at desired coordinates with a high density, precision, and resolution. Similarly, like other bioprinting modalities, laser-based bioprinting is also divided into many categories, out of which the most used are laser-guided direct writing, SLA, and DLP.[22]

Light-based bioprinting is another type of bioprinting method that is considered to be under the laser-based techniques that employ various ways that utilize light to induce polymerization to photopolymerizable bioinks or biomaterials in order to perform layer-by-layer deposition. The most common is DLP method which uses digital micromirror devices (DMDs) or liquid crystal display that projects light over photosensitive biomaterials that in turn allows for the layer-by-layer forming of organic cellular structures.[32] The DMD, which is coupled to a light projector, projects a 2D image of each layer onto the bioink, hardening or crosslinking it when exposed to light.[32b] This method is re-

peated for each layer until the desired structure is complete. DLP bioprinting has great resolution, fast printing speeds, and compatibility with a variety of biomaterials, making it ideal for tissue engineering and regenerative medicine applications.[33] Another light-assisted bioprinting technique is the less common two-photon polymerization (2PP) bioprinting technique, where femtosecond laser is utilized to accurately direct light onto a photosensitive material, causing polymerization only at its focal point. This causes the construction of high-resolution structures with sub-micrometer precision. Although not as widely employed in bioprinting as in other applications, 2PP has the ability to produce sophisticated microstructures and scaffolds for tissue engineering.[34]

2.2.2. Scaffold-Free Bioprinting

Scaffold-free bioprinting assembles the smallest unit "single-cell suspension, spheroids, tissue strands or cell sheets," by combining them to build larger constructs and it depends on the cells creating the extracellular matrix.[35] Biocompatibility being one of the deciding factors for choosing a bioink for a specific bioprinting application, can be greatly increased when using only cells as the bioink without mixing it with a biomaterial such as hydrogels in scaffold-free bioprinting. The reason for this is the usage of patient-derived cells that can lead to the creation of fully autologous tissue constructs. Moreover, spheroids-based methods reduce or eliminate cell damage produced via shear stresses from nozzle extrusions. A common limitation of this method is that the cell units do not produce stable solid structures or assemblies and chemical means are required for intercellular adhesions. Intercellular adhesions or structural cohesions require additional time and are dependent on cell type. Furthermore, the biomechanical properties of scaffold-free tissue constructs are less predictable as opposed to scaffold-based.[36]

2.2.3. VBP

VBP or CAL is a relatively recent bioprinting classification, having been first introduced in 2017.[37] that has sought to capitalize on the printing speed and geometrical accuracy of 3D biostructures. It uses a similar principle of light-based bioprinting methods of photopolymerization but differs as the fabrication is rapid and simultaneous and not the layer-by-layer process of light-based methods.[38] In VBP, a 3D light dose is applied to a volume of photo-responsive polymer material, resulting in synchronous polymerization throughout the volume.[39] This enables the layerless creation of centimeter-sized constructions, considerably lowering printing time compared to traditional layer-by-layer methods. Furthermore, VBP frequently employs spatially modulated light sources that encode visible light with tomographic back projections, allowing for fine control over the printing process and the development of intricate 3D cellular structures.[40]

2.3. Biomaterials

The human body has miraculous healing capabilities however, this regenerative ability is limited by time, the size of the injury, and available nutrients.[41] Historically, the application of biomaterials had been the replacement of damaged tissues, like fracture fixation of bone, the development of artificial heart valves, dressing of wounds, etc.[42] Recently, biomaterials are being researched for bioprinting applications to be used as a building block for bioink.[41] Biomaterials can be defined as a category of materials that can interact and interface with biological systems. Biomaterials can play an important role as a replacement for a part or a function of the human body safely and reliably. Moreover, rheological properties such as viscosity, yield stress, etc. can influence the shape and quality of tissue constructs, and therefore, choosing a biomaterial for a specific application requires research before printing.[43]

Biomaterials can be classified into three major categories based on their chemical composition: ceramics, composites, and polymers.[44] The composite type is a combination of both ceramics and polymers. For bioprinting, the most important class of biomaterials are polymers, mainly because of their similarities with connective tissues, and they are widely used in both tissue engineering and regenerative medicine. The polymer class is further classified into two main groups: natural and synthetic.[45] Natural polymers such as alginate, collagen, chitosan, agarose, etc. are preferred over synthetic polymers due to biocompatibility, biodegradability, and other crucial characteristics.[46] Synthetic polymers such as polyester, polyether, polyethylene derivatives, polycarbonates, etc. can be modified versions of natural polymers or completely altered via tailored characteristics such as mechanical constraints, shape, reproducibility, and degradability.[41]

2.4. Bioink

Bioink differs from biomaterials as it can be defined as a specific formulation of cells that are required for a bioprinting technology and it might contain biomaterials or biologically active components.[47] The bioink formulation, as depicted in **Figure 2a**, plays a pivotal role in bioprinting, offering a nuanced understanding of the diverse polymer configurations essential for constructing intricate tissue constructs.[48]

For bioprinting, the bioink can be divided into two major types: scaffold-based, and scaffold-free.

(a) Scaffold-based bioink: In scaffold-based bioink, cells are loaded into biomaterials such as hydrogels which allow cell proliferation and the growth of tissue constructs.[49]

(b) Scaffold-free bioink: In scaffold-free bioink, only cells in different encapsulations such as tissue spheroids, cell pellets, tissue strands, etc., are 3D printed without a biomaterial.[50] In this way, the risk of infection, immune response, and disease transmission can be avoided, and other problems related to scaffold-based bioink can be fundamentally solved.[51] The choice of bioink is also dependent on the application and fabrication techniques. Specifications for bioink can range from rheological properties such as shear-thinning, thermal conductivity, mechanical, etc. to qualities such as cell attachment, proliferation, cell growth, etc.[52]

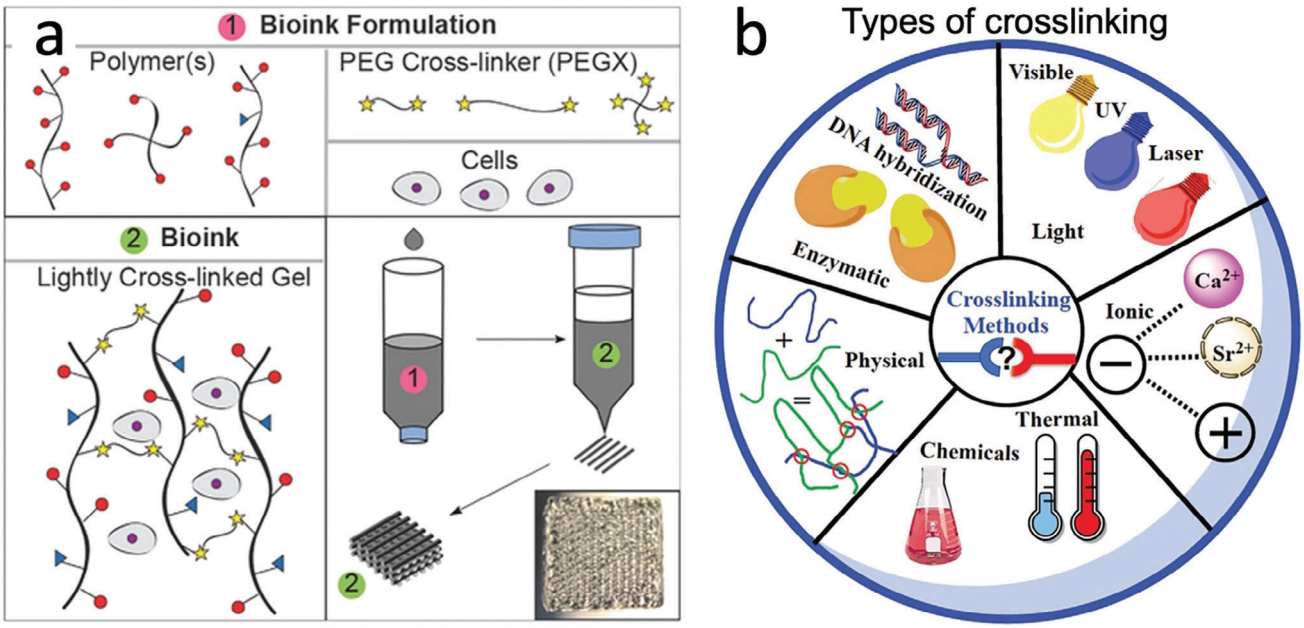

Figure 2. a) Polymer or polymer mixtures, exemplified by gelatin, 4-arm PEG amine, and gelatin methacrylate, can exist in linear, branched, or multifunctional forms. The representation includes amines (red circles), methacrylate groups (blue triangles), and SVA groups of PEGX (yellow stars), where PEGX can be linear or multiarm with varying chain lengths. Optionally, cells can be integrated by blending them with polymers and PEGX to create the bioink. The printing process involves mixing PEGX, with or without cells, into the polymer solution, loading it into the printing cartridge, and 3D printing multilayer structures after gel formation. Adapted with permission.[48] Copyright 2015, Wiley-VCH. b) Highlights various crosslinking methods employed in the 3D bioprinting of hydrogels. Reproduced with permission.[54] Copyright 2020, Wiley-VCH.

2.5. Crosslinking Techniques

Another critical issue is crosslinking, which is a stabilization process in which one polymer chain bonds with another polymer chain that converts a liquid polymer into a solid or solid-like structure, resulting in losing their ability to move freely as an individual chain.[53] An appropriate crosslinking mechanism for different bioprinting modalities is crucial for achieving the cellular behavior of loaded live cells, better printability, and biomechanical stability for printed structures.[54] Crosslinking strategies have two major categories: physical crosslinking and chemical crosslinking, which are further divided into subcategories.[55] Physical crosslinking is inter-molecular interactions such as ionic bonding, hydrogen bonding, polymerized entanglements, etc.,[56] while chemical crosslinking includes photopolymerization,[57] enzyme-induction,[58] click reactions, etc.[59] Figure 2b shows various crosslinking methods employed for the bioprinting of hydrogels.[54]

3. Computational Analysis of Bioprinting

3.1. History of CFD

CFD has been used since the late 1950s using computer software for 3D transient applications and for incompressible flow.[60] The first attempt at a modern-day CFD problem was done by Lewis Fry Richardson in 1922 using around 60 000 "human calculators" around a globe that resembled Northern Europe to predict the weather and analyze the fluid flow across certain areas. His method was the basis for modern-day CFD, laying the foundation of cells—"human calculators"—and numerical instability as his method had to make sure that the cells performed the calculations at the same time.[61]

Since then, CFD has been used in many applications, as mentioned in the introduction to this paper, such as the aerospace and automotive industries. CFD has been a key element in R&D in many research fields, namely, bioengineering, environmental engineering, biomedical applications, and HVAC for industrial applications. The engineering applications that have been considered in the aforementioned fields are cavitation prevention, simulation of rotating machine elements in machinery, simulation of laminar and turbulent flow, aerodynamic simulation, and heat transfer simulation, to mention a few.[62]

One of the reasons for this review is to discuss the CFD aspect of bioprinting, an AM method for tissues. CFD has been used in bioprinting to simulate the rheological properties of bioink, especially the shear stress at the end of the nozzle,[63] the diffusivity of the final scaffold,[64] as well as the cell viability, which is negatively affected because of the shear stresses toward the end of the nozzle, which in turn is caused by the velocity gradient toward the end of the nozzle.[65] Therefore, nozzle design and design parameters will also be discussed later on.

3.2. Analysis of Different Types of CFD Software and Their Uses with Bioprinting

Bioprinting encapsulates many areas and some of them use CFD to make analyses such as the printability of the inks,[66] the cell viability,[22,67] and nozzle design.[12,65,68] The CFD method incor-

Table 1. Summary of CFD software's for bioprinting.

Name	Purpose	Type of bioprinting method	Studied rheological properties	Reference
IPS IBOFlow	To simulate the flow behavior of the bioink and predict the final shape	Extrusion	Viscosity, flow rate, pressure	[63]
COMSOL Multiphysics/COMSOL 4.0a	To study the diffusion in scaffold design and how the pore structure affects it	Extrusion	Effective diffusivity	[64]
		Droplet	Flow rate, viscosity, density	[69]
COMSOL Multiphysics 4.2	To simulate the flow in the microfluidic channel	Extrusion	Viscosity, shear stress	[70]
COMSOL Multiphysics 5.2a	To investigate the effect of shear stresses in the printing geometry (conical/straight nozzles) and the cell viability	Extrusion	Process-induced shear and extensional stress	[71]
		Extrusion		[72]
		Extrusion	Shear stress, pressure, temperature, velocity	[73]
	Simulate fluid flow inside the needle on the printing profile to investigate velocity field and mass flow rate	Droplet		[74]
		Droplet	Shear stress, viscosity, pressure, concentration	[75]
	To examine the flow of non-crosslinked gelatin in the needle	Droplet		[76]
	To identify the shear stresses and pressure drop that cells experience in the bioprinting process		Shear stress, pressure, viscosity, flow rate	
	To improve drug transport in the intraperitoneal region during peritoneal metastasis		Pressure, concentration, solid stress	
	To study the 3D matrix profile at the bottom channel and the top channel		Concentration, mass flow rate, momentum	
	Devising a mathematical model to simulate the mass and momentum transport in the microfluidic device			
ANSYS Workbench/ANSYS Fluent/ANSYS CFX	To examine the maximum wall shear stress in three different nozzle designs: tapered conical, conical, and cylindrical	Extrusion	WSS, mass flow rate	[12]
		Extrusion	Viscosity, storage modulus, loss modulus, shear stress, flow rate	[77]
		Extrusion		[78]
	To study the wall shear stress in conical and straight-shaped nozzle	Extrusion	Shear stress, concentration	[79]
		Droplet	Shear stress, pressure, velocity, shear rate, dynamic viscosity, mass flow rate	[80]
	To simulate the flow hemodynamics in pulmonary artery geometries	Extrusion		[81]
		Scaffold-free		[82]
	To identify the pressure gradient and maximum shear stress at the top of the nozzle to verify analytical calculations	Laser	Shear stress, velocity, viscosity	[83]
		Laser	Shear stress, porosity	[84]
	To study the effect of shear stress in piezoelectric print-head used in drop-on-demand (DoD) bioprinting method		Force, pressure, shear stress, flow rate, oxygen distribution	
			Velocity, shear stress	
	To investigate porosity in scaffolds and the relationship between pore structure and scaffold maximum shear stress		Velocity, length of jet, mass flow rate, droplet size	
	To improve tissue design and bioreactor implementation			
	To analyze flow in a recanalized model of aortopulmonary collateral arteries that are affected by Tetralogy of Fallot			
	To assess the growth and development of flow and the outcome of printing, that is, the printing quality			
FLOW 3D	To study droplet formation in inkjet printing modality	Droplet	Density, viscosity, surface tension, velocity	[85]
OpenFOAM	To optimize nozzle design and identify all major printing factors that affect the printing process	Extrusion	Shear stress	[68]
		Extrusion	Shear stress, porosity, surface roughness	[86]
	To investigate the effect of shear stress prevention methods to improve cell viability	Extrusion		[13]
	To investigate the flow in the printer head and the deposition to identify the relationship between printing parameters and hydrogel behavior		Viscosity, flow rate, pressure, shear stress	

(*Continued*)

Table 1. (Continued)

Name	Purpose	Type of bioprinting method	Studied rheological properties	Reference
ABAQUS	To study the mechanical properties of hydrogels at various cell densities and types of cell distributions, that is, corner, cluster, and random	Extrusion, droplet, laser	Viscosity, cell density, shear stress, shear modulus	[87]
Gerris	To examine the viscous boundary layer inside the droplet and the formation of the rim	Droplet	Velocity, viscosity, surface tension	[88]
SOLIDWORKS flow simulation	To investigate the syringe cooling system used in the printer	Extrusion	Pressure, flow rate, viscosity	[89]

porates the pre-processing, solving, and post-processing system, which are used congruently by different software and further methods. This system, along with different discretization methods, is used by different software to analyze different aspects of different printing methods. Different types of CFD software and the methods they employ are exclusive to the application they are to be used for. **Table 1** summarizes the different types of CFD software, their purposes, printing method which employs them, and studied rheological properties.

In **Figure 3**, a flow chart of CFD is shown depicting the detailed steps of the CFD methodology for Fluent. It is divided into three major segments, pre-processing, solver, and post-processing. The development aspect of the CFD bundle is mainly seen in the pre-processor. The solver segment focuses on the constraints such as boundary selection and model selection. The results of these constraints and diversions due to course plots are shown in the post processor.[90]

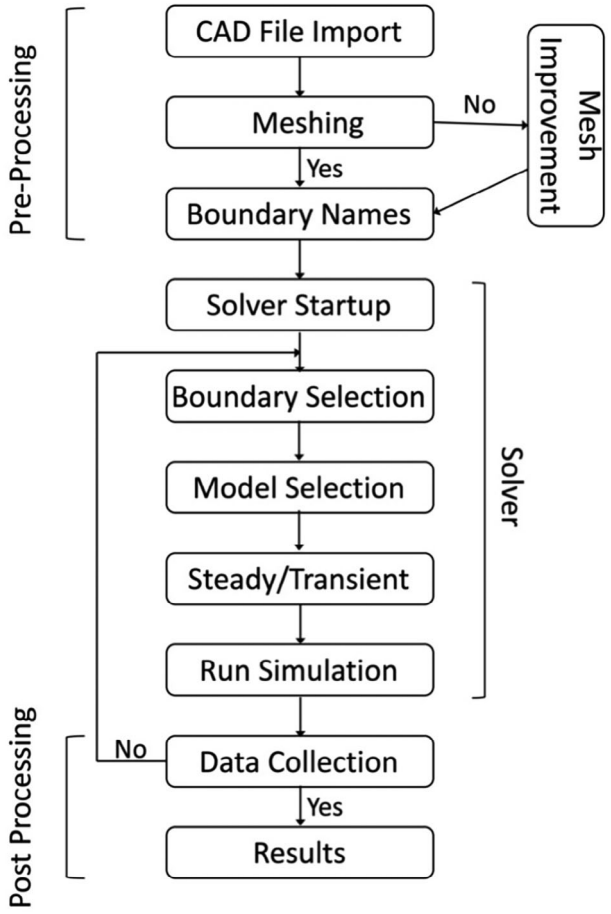

Figure 3. The detailed CFD methodology with the pre-processing, solver, and post-processing.[90]

3.3. . CFD Method for Bioprinting

The pre-processor determines the number of elements, defines the domain and fluid properties, assigns the initial physical states, and selects the boundary conditions that are to be used in the simulation. The solver integrates the governing equations over all the control volumes that were defined using the number of elements and nodes at the pre-processing stage. The solver then converts the differential equations that are to be integrated into algebraic equations—which is called discretization—that are then solved linearly by iterations. The solver also employs existing numerical methods for the specific problem which uses the appropriate parameters to calculate a suitable solution. The post-processor involves charts, surface, vector and contour plots, and flow animation, in order to visualize the results, and later analyze them.[91] Moreover, CFD is used for bioprinting applications to reduce costs and with modern computing, highly accurate results can be observed for the simulations. It is worth mentioning that CFD for bioprinting mainly participates in printability and cell viability.[92]

3.3.1. . CFD for Extrusion-Based

Material extrusion, a filament-based bioprinting process, is widely adopted for its high efficiency, versatility with various biomaterials, and ease of execution. In this process, filament morphology is of paramount importance as it forms the basic building blocks for printed 3D structures and it determines the printing resolution, surface quality, and structural integrity of the final product. CFD for extrusion-based bioprinting has been tremendously useful in designing the nozzle, investigating the rheological properties of the bioink, such as velocity, pressure, and shear stress, and analyzing the results which are the printing parameters such as the printability, and cell viability.[93] and the shape fidelity.[73,94] These parameters are further investigated later in this review. **Figure 4** shows an example of analytical and CFD analysis for extrusion-based bioprinting. The geometry of noz-

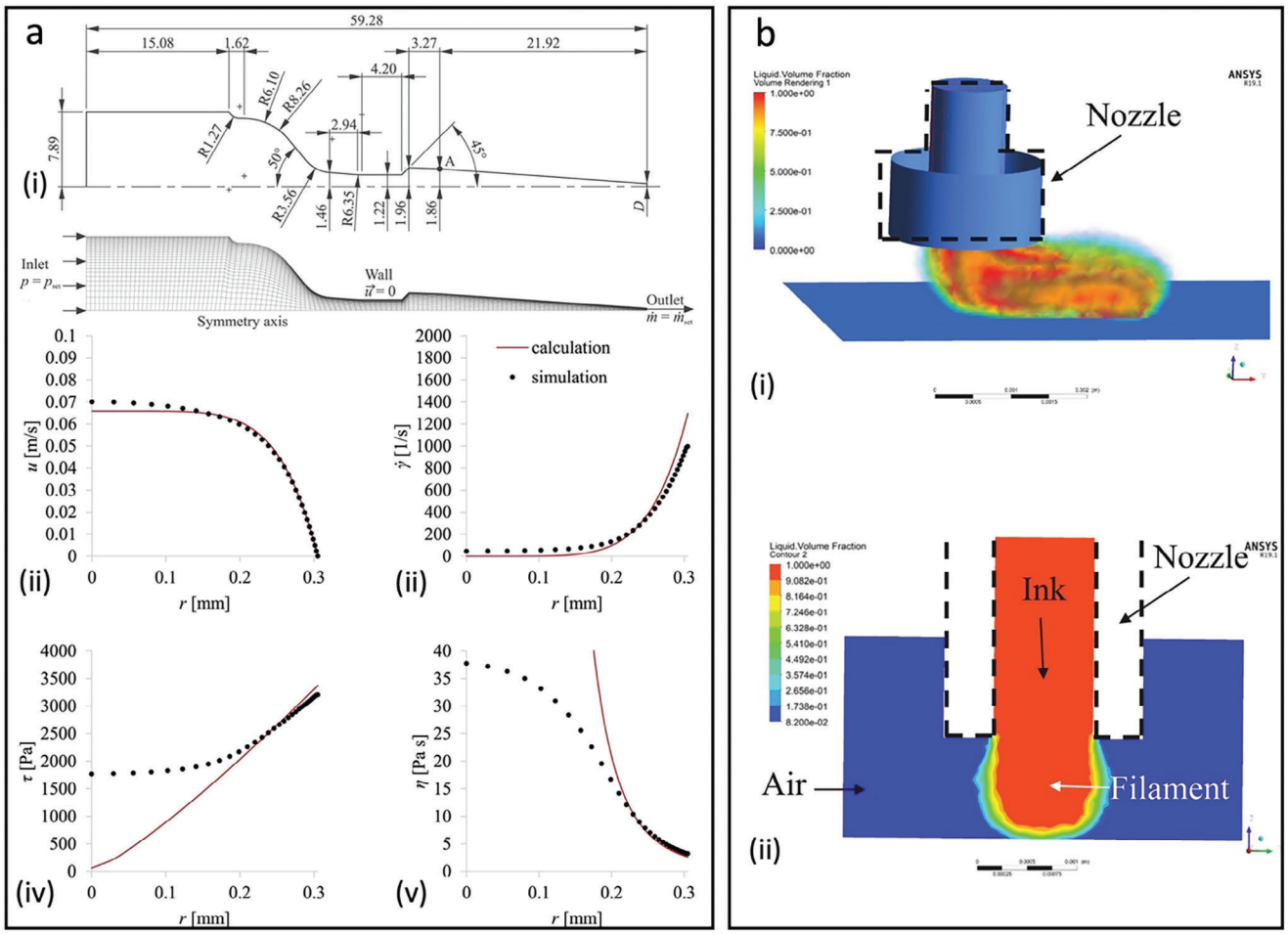

Figure 4. CFD for extruding-based bioprinting. a-i) The geometry and the mesh and boundary conditions of a 2D axisymmetric CFD model. The dimensions are in mm. ii–v) For a printing needle with an outlet radius diameter $D = 0.61$ mm and mass flow rate $\dot{m} = 12.37$ mg s^{-1}, distribution of selected flow parameters obtained from analytical calculation (red line) and CFD simulation (dotted black line) are graphed. ii) Axial velocity, iii) shear rate, iv) shear stress, and v) dynamic viscosity. Adapted with permission.[79] Copyright 2020, IOP Publishing. b-i) Front view of a simulation of filament deposition and ii) side view of a simulation of filament deposition. Adapted with permission.[95] Copyright 2021, Elsevier.

zle design was analyzed with Ansys Fluent as well as axial velocity, shear rate, shear stress, and dynamic viscosity.[79] In another study, CFD was used to study the printing performance of a jammed gelatin microgel-based composite ink during extrusion, with a focus on the filament cross-sectional morphology and the impact of the ink's yield stress on printability (Figure 4b).[95]

3.3.2. . CFD for Droplet-Based

Droplet-based bioprinting techniques require CFD for analyzing different parameters as well, such as viscoelasticity[96] and fluid flow, especially in microfluidic channels.[69] Moreover, microfluidic advancements such as the tumor-on-chip system have been subject to CFD simulations as well to investigate the movement of substances near the tumor in the system.[74–76] Droplet formation, for example, was simulated using FLOW 3D software for different bioink formulations as shown in **Figure 5**[85] Their results were validated by experimental results of imprinting bioinks on different substrates. Their simulation studies demonstrated that bioinks with higher viscosity necessitated higher velocities for effective jetting.

3.3.3. . CFD for Laser-Based

SLA, a common type of laser-based bioprinting technique, has been in use for various biomedical applications. Many studies show that CFD was used to analyze the dynamics of blood flow (hemodynamics) on bioprinting structure that was fabricated utilizing the DLP technique.[78,83] Tomov et al.[78] prepared a study in which a model utilized an in vitro platform incorporating DLP bioprinted bifurcated pulmonary arteries (PA), seeded with human endothelial cells and perfused at physiological flow rates, to simulate vascular anastomosis and aid in procedural planning to reduce restenosis, with CFD employed to quantify flow velocity and wall shear stress (WSS) within the bioprinted arteries, identifying regions prone to stenosis. **Figure 6**a shows the dynamics of PA constructs involved in fluid flow patterns crucial for optimizing bioprinted vascular structures. CFD simulations, using

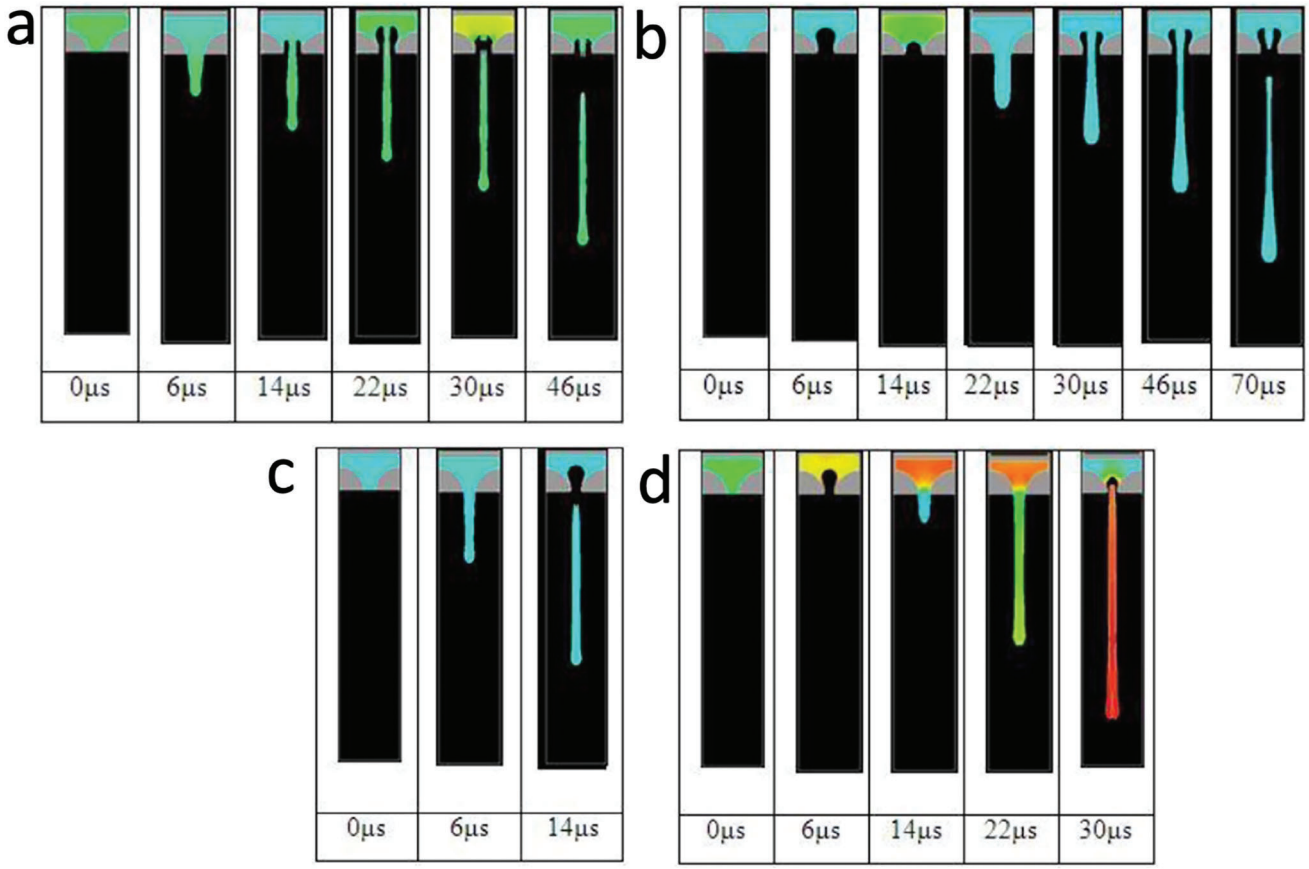

Figure 5. CFD for droplet-based bioprinting. Formation of droplets and the trailing effect observed in a) BSA bioink 1 (BSA + No modifier); b) BSA bioink 2 (BSA + CMC); c) BSA bioink 3 (BSA + Triton X-100); d) BSA bioink 4 (BSA + CMC + Triton X-100). Adapted with permission.[85] Copyright 2016, Elsevier.

Ansys FLUENT solver, analyze flow velocity, pressure distribution, and shear stress as the study explored the effects of conduit diameter and angle on flow hemodynamics, providing insights into different design configurations to optimize flow patterns in PA constructs. The same group conducted another CFD study for a DLP bioprinted patient-specific human heart model, as seen in Figure 6b.[97] The bioprinted human heart model of the human embryonic and fetal left ventricle was analyzed experimentally using ultrasound and 4D MRI and computationally using CFD, focusing on flow velocity and shear stress. They obtained consistent results with both the experimental and CFD studies.

Moreover, the 2-photon polymerization (2PP) technique was also used to create microfluidic chip devices, where CFD was employed to analyze the flow of the medium within the device.[98] Another type of laser-based technique was laser-induced forward transfer (LIFT), where the jet flow was optimized using CFD.[84] CFD simulation stands as a potent and effective tool that aids the design process in laser-assisted bioprinting method as well, minimizing the labor-intensive nature of experimental endeavors. Through the integration of CFD with bioprinting experiments, a sample of study shown in **Figure 7**, it becomes possible to predict distinctive characteristics of jet and bubble formation in the initial stage of the study.[84] This, in turn, guides the bioprinting process, improving printing quality by suggesting optimal printing parameters. This recommendation is derived from the correlation between the jet regime and the resulting printing patterns on the substrate.

3.4. Application of CFD

3.4.1. Printability

The printability of the bioinks has been subject to research, with studies covering the different types of bioprinting methods: extrusion-based, droplet-based, and laser-based. For the extrusion-based printing method, printability is defined as the suitability of the bioink that is to be used in terms of certain parameters, such as its extrusion capability, shape fidelity, and accuracy.[66b] For droplet-based or inkjet bioprinting, printability refers to the accuracy of the droplets that are produced in the air.[99] Laser-based bioprinting uses printability to define how well the uniformity of the jet is produced so that it can form accurate droplets and settle them onto the substrate.[100]

Printability is defined by certain parameters such as extrudability, strand printability, integrity factor, irregularity, and pore printability.[66b,101] The extrudability is the capability of the extrusion to be conducted, thereby meaning the pressure that is least

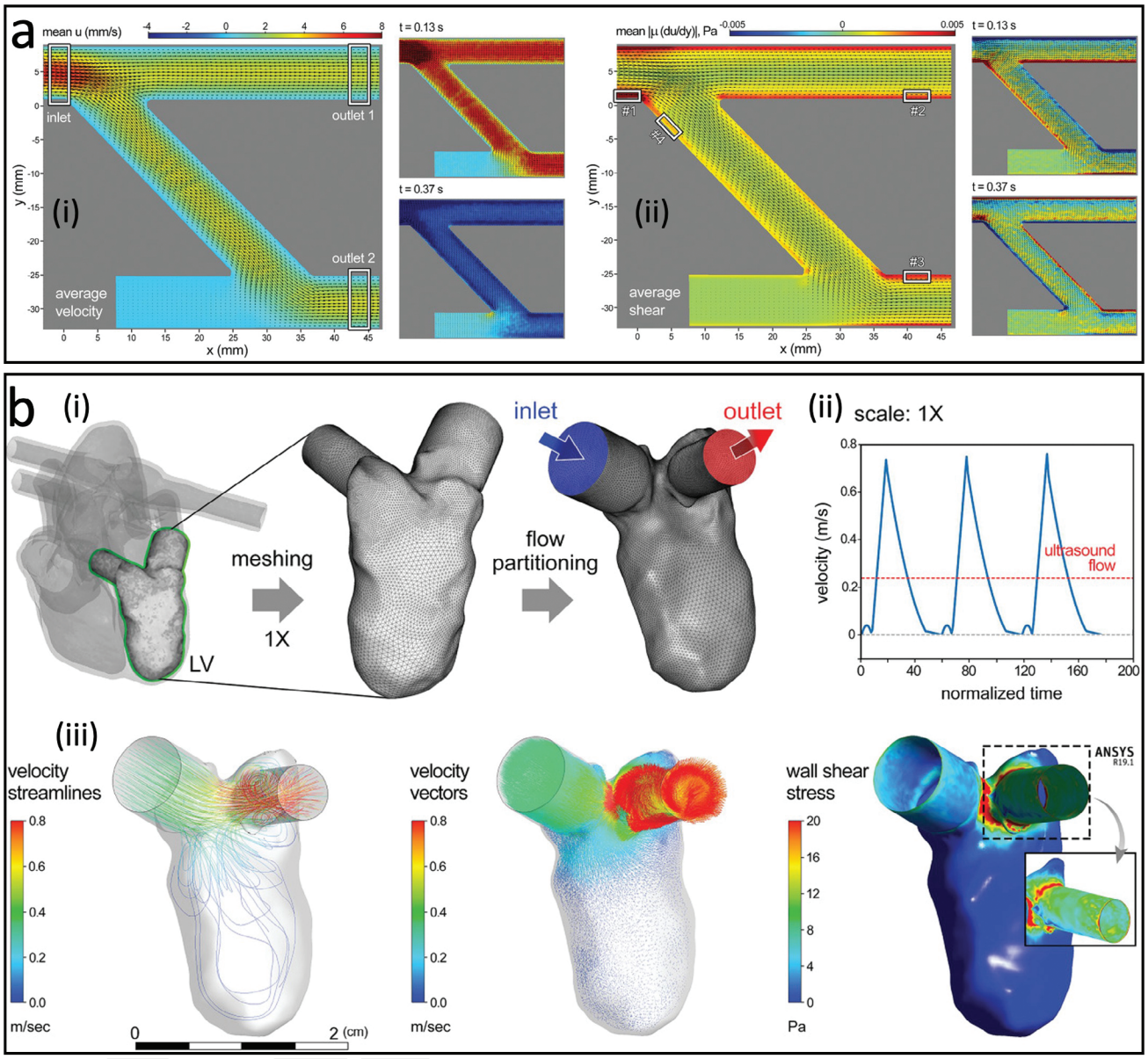

Figure 6. CFD for DLP-based bioprinting. a-i) Averaged flow patterns produced over a single peristaltic flow cycle (left) and flow patterns at two specific time points ($t = 0.13$ s, top right and $t = 0.37$ s, bottom right). ii) Averaged shear patterns generated during one cycle of peristaltic flow (left) and shear patterns at two specific time points ($t = 0.13$ s, top right and $t = 0.37$ s, bottom right). Adapted with permission.[78] Copyright 2021, Wiley-VCH. b) Conversion of a patient-specific 3D printed fetal left ventricle geometry into a i) meshed boundary for CFD analysis conducted using an ii) anatomically suitable flow wavefront. iii) CFD outcomes showcased velocity and wall shear stress at peak flow. The inset in (iii, right panel) provides magnified views of peak wall shear stress, exhibiting higher values at the aortic outflow tract. Adapted with permission.[97] Copyright 2021, Wiley-VCH.

required to extrude the material at the specific flow rate. Strand printability is a factor in determining the comparison between printed strand diameters and software-generated strand diameters. The strand diameter is given by:

$$D_s = \sqrt{\frac{4Q_t}{\pi V_n}} \quad (1)$$

where D_S is the strand diameter, V_n is the needle speed and Q_t is the volumetric flow rate.[66b,101b]

The strand printability is then given by:

$$\text{Strand printability} = \frac{\text{Experimental strand diameter}}{D_s} \times 100 \quad (2)$$

The integrity factor compares the thickness of the printed material (scaffold) to the control (designed) material. The irregularity index examines the integrity factor in 3D, where the outer geometry of the printed material is compared to the control ones in the *X*–, *Y*–, and *Z*–directions.[66b] Pore printability is the index factor that examines the internal geometry as opposed to

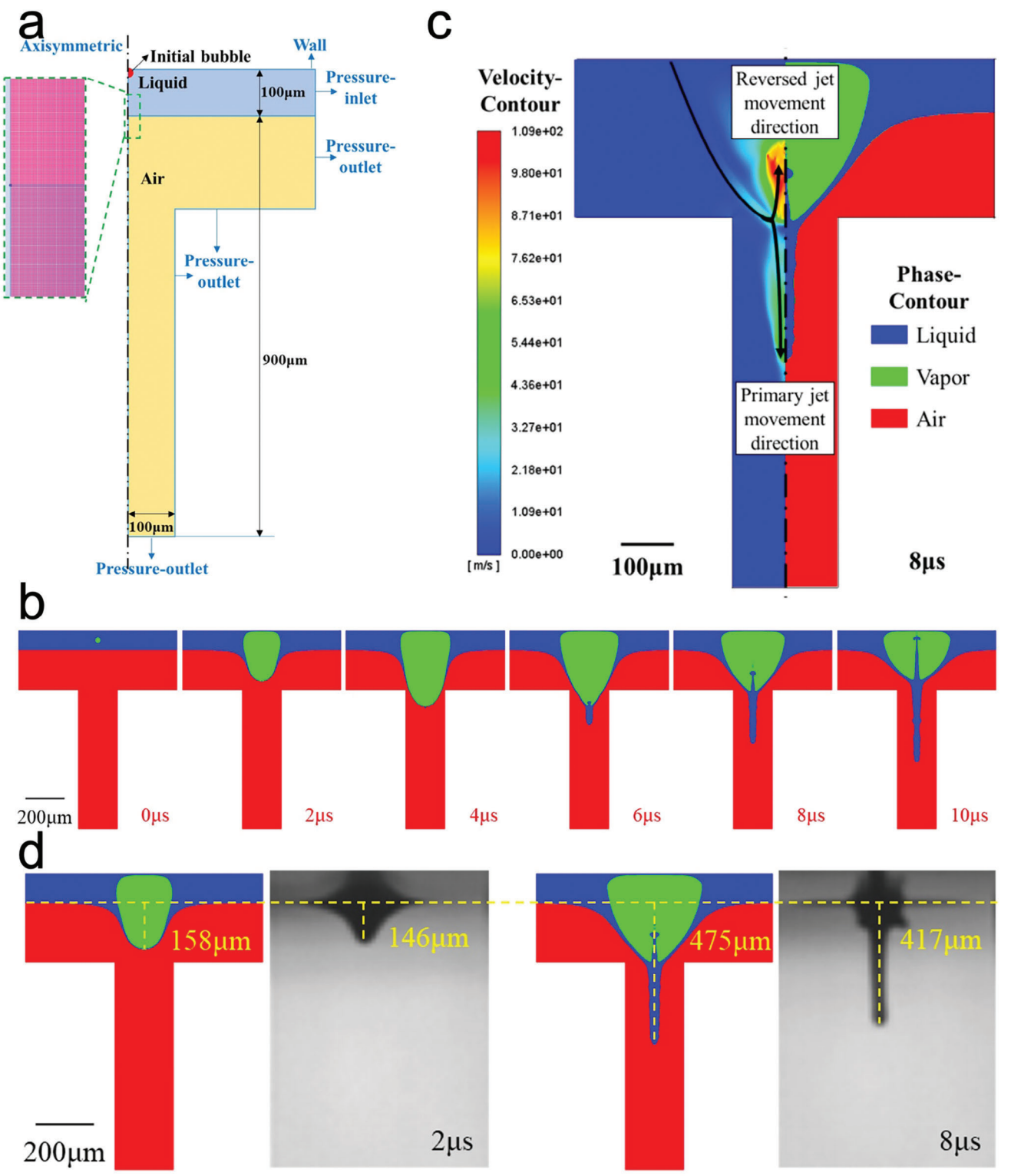

Figure 7. CFD for laser-assisted based bioprinting. Simulation of jet flow is depicted in the following manner: a) Schematic illustration of the simulation model's geometry and meshing configuration. b) Visualization of the jet flow featuring a 100 μm thickness 65% glycerol layer and 717 mJ cm^{-2} laser fluence. c) Presentation of the velocity of the jet flow at 8 μs. Reproduced with permission.[84] Copyright 2021, arXiv. d) Comparative analysis with experimental results from a previous study.[100]

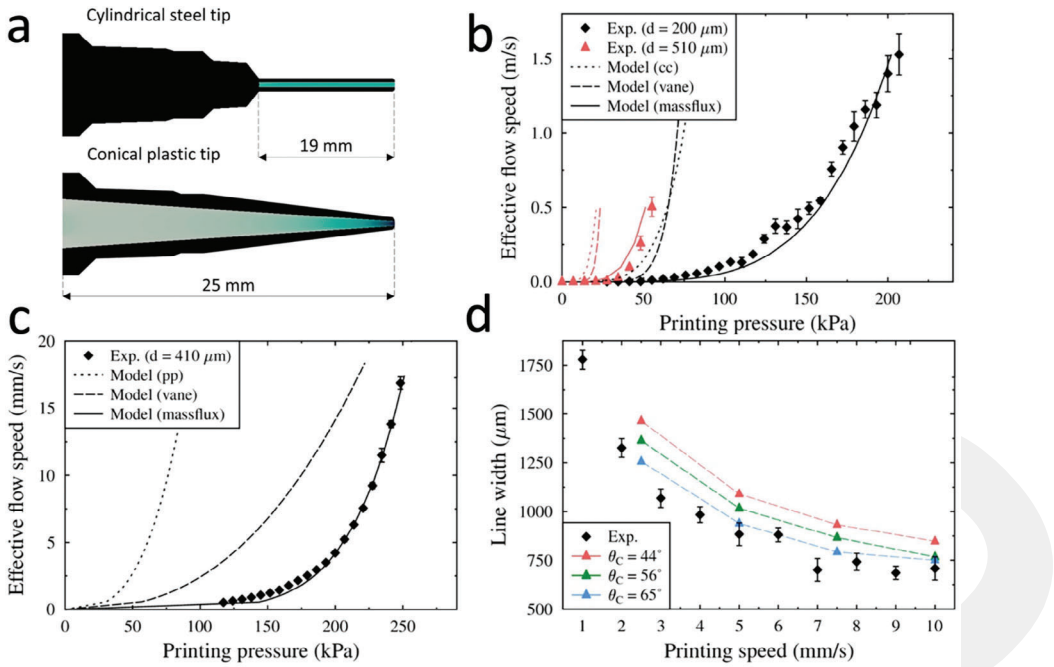

Figure 8. CFD for printability. a) Nozzle geometries, top: the cylindrical steel tip and bottom: the conical plastic tip. b) Comparison of experiments results and CFD simulations showing effective flow speed within the nozzle as a function of operating pressure for the TCNF hydrogel and c) for the ATG50 hydrogel. d) Line thickness as a function of printing speed for the TCNF hydrogel. Adapted with permission.[13] Copyright 2017, American Chemical Society.

the integrity factor and the irregularity index. It compares the pores printed on the scaffold to the ones in the design.[66b,101a] CFD is an effective tool to estimate the printability of bioinks in terms of varying perspectives such as printing speed, nozzle geometry, dispensing pressure, temperature, and rheological characterizations.[14,63,65,102] A study used CFD analysis to anticipate the printability, as shown in **Figure 8**.[13] The printing flow rate, pressure, print speed, and line thickness were computationally analyzed and experimentally validated. It proves the power of CFD in improving printability.

3.4.2. Cell Viability and Nozzle Design

Cell viability and nozzle design are other parameters that can be analyzed using CFD for bioprinting. Literature has shown the factors affecting cell viability when it comes to bioprinting.[14,68,73,80,103] We are investigating CFD applications on nozzle design with cell viability because one of the major factors affecting cell viability is the nozzle geometry. It is also the same in the literature: CFD analysis of nozzle geometry and printing parameters such as nozzle radius, length, speed, and flow rate have been conducted while considering cell viability. Shear stress stands out as the most critical parameter affecting cell viability in the context of nozzle design, especially within extrusion-based bioprinting.[65,80,104] The shear stress values were compared against the cell viability values from literature.[79,104b,105] which agreed with the negative correlation of maximum shear stress and cell viability. Therefore, the nozzle design was optimized, taking into account the shear stress. **Figure 9a** depicts a CFD simulation that was conducted to investigate potential correlations between maximum and/or average shear stress within the printing geometries (cylindrical and conical needles) and their impact on cell survival and spreading.[70] There is another CFD application regarding analyzing the fluid velocity in the nozzle for two different geometries, as shown in Figure 9b.[77b] Chand et al.[12] investigated three common nozzle designs: conical, tapered conical, and cylindrical. They identified the shear-thinning properties such as nozzle geometry, nozzle diameter, inlet pressure, and bioink fluid characteristics (Figure 9c). In another study, conical nozzles were compared with blunted nozzle designs, and their radii were considered to assess the maximum wall shear stress (MWSS). The MWSS for the blunted nozzle is at its highest in the middle of the nozzle, but at the tip of the conical nozzle. The other parameters that affected the cell viability were the power-law index, the nozzle length, and the material properties, which were simulated by CFD (Figure 9d).[68] The accuracy of simulation results was validated with a comparison of analytical results for simplified geometries by Ansys PolyFlow.[106]

Figure 10 shows a study in which nozzle geometry and shear stress effects on cell viability were investigated with experimental and computation analysis.[72] Contrary to conical needles, which require high pressure only at the nozzle tip, cylindrical nozzles have a consistent radius and require constant pressure throughout for extrusion, resulting in a longer region of maximum shear stress. As a result of the longer transit time in the area of high shear stress, this indicated that cell death was higher in the

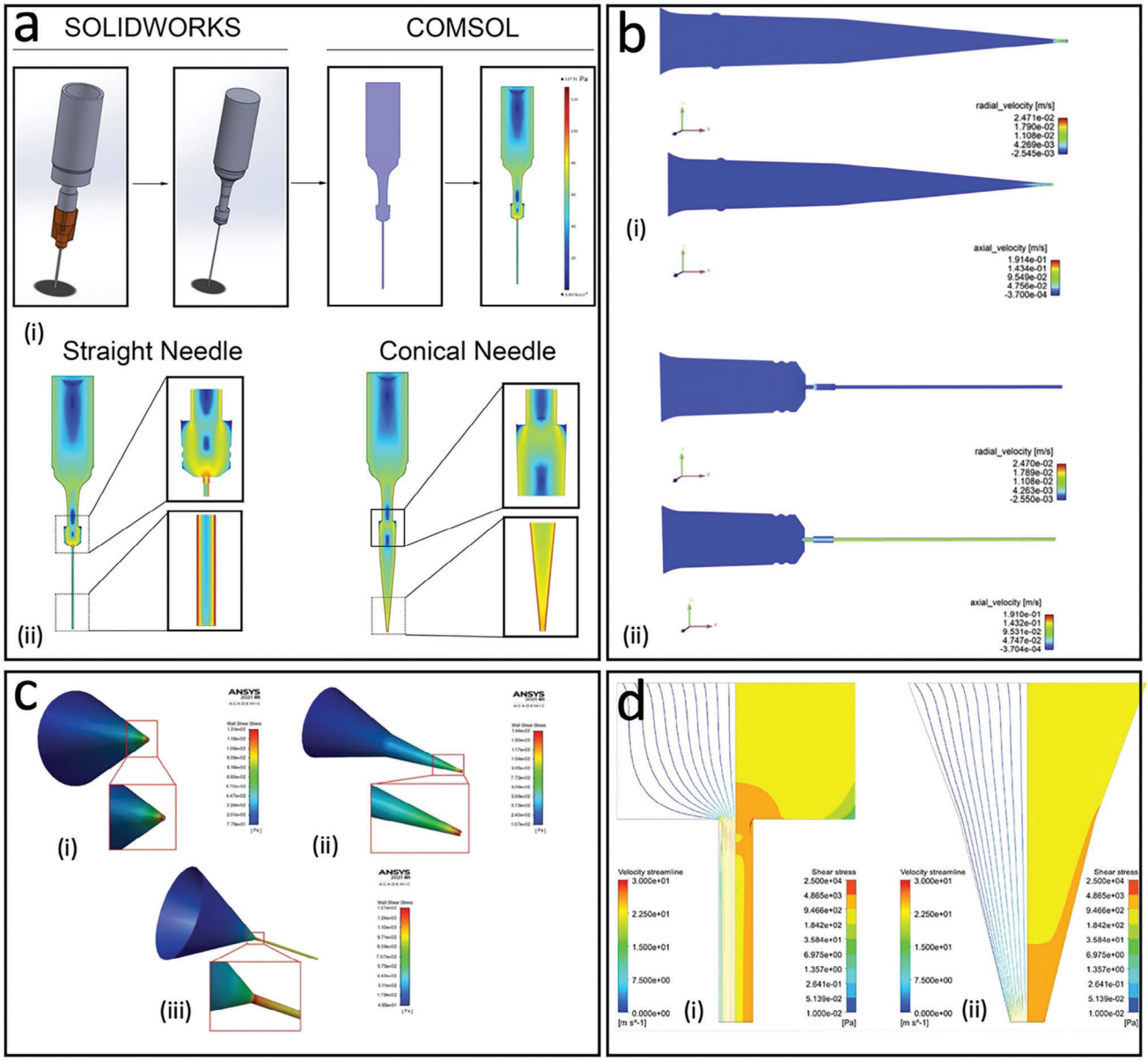

Figure 9. CFD for nozzle design. a-i) Fluid volume models were generated from 3D CAD models using SOLIDWORKS and simulations in COMSOL. ii) Regions of high shear stress are highlighted by the red/orange color, revealing noticeable distinctions between the straight and conical needle geometries. Adapted with permission.[70] Copyright 2017, Springer Nature. b-i) Simulation of radial and axial velocities of bioink through conical nozzle, ii) through tubular nozzle (D = 200 µm, L = 13 mm). Adapted with permission.[77b] Copyright 2020, Elsevier. c) CFD results of wall shear stress for i) tapered conical, ii) conical, and iii) cylindrical nozzle with outlet diameter 0.3 mm. Reproduced with permission.[12] Copyright 2022, ACCScience Publishing. d) Velocity streamline profile (left part) and shear stress distribution (right part) of alginate hydrogel simulated at 340 kPa inlet pressure i) for cylindrical nozzle design and ii) for conical nozzle design. Adapted with permission.[68] Copyright 2021, Frontiers.

cylindrical nozzle. In a study of CFD simulation via COMSOL 4.0a software, a comparison was made between conical and cylindrical needle geometries concerning their impact on cell viability. The simulation results revealed that conical-shaped needles generated the highest shear stress. However, cells exhibited resilience to this stress within a confined region near the needle's outlet. In contrast, cylindrical needles produced a lower shear stress peak, but it was distributed over a longer pathway along the needle (see Figure 10).[72]

3.4.3. Artificial Vessels

Another application of CFD for bioprinting is the shear stress analysis of the walls of 3D biofabricated blood vessels. Because blood vessel plays a crucial role in transporting nutrients and oxygen and maintaining homeostasis in the human body.[107] Fabricating artificial vessels is necessary to overcome vessel injuries therefore, 3D bioprinting stands as an innovative technology with the capacity to revolutionize the field by constructing intricate

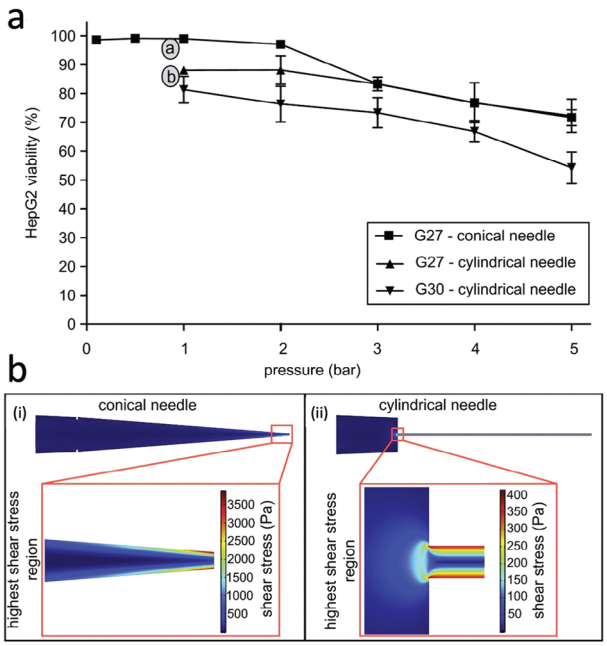

Figure 10. CFD for cell viability. a) Experimental results of cell viability during the printing process as a function of the applied inlet pressure and needle type. b) Heat map of the shear stress different nozzle geometries i) for a conical needle and ii) for cylindrical needle. Reproduced with permission.[72] Copyright 2014, Elsevier.

multicellular structures. There are several variables, including vessel diameter, wall thickness, wall pressure, flow velocity, flow viscosity, and temperature, that can have an impact on the shear stress of blood vessel flow in the biofabrication process. However, it is extremely hard to control these factors during the fabrication. Therefore, CFD is the tool that helps to pre-estimate or optimize these factors before doing biofabrication.[108] In a study, WSS distribution was simulated by COMSOL. Through CFD simulation, the vessel exhibited notable perfusable and mechanical properties across different flow velocities, flow viscosities, and temperature conditions (**Figure 11a**).[109] In another study, The WSS profiles were simulated with parameters mimicking circulating tumor cell (CTC) perfusion experiments in laminar flow, highlighting the impact of channel architecture on flow dynamics (Figure 11b).[110] It provides valuable insights into WSS and laminar flow during CTC perfusion. The quiver plot illustrates laminar, non-turbulent flow at a specific branching point.[110] This data contributes significantly to the comprehensive analysis of CFD applications in bioprinting, shedding light on the intricate fluidic aspects critical for successful tissue engineering.

3.4.4. Microfluidic Chips

Microfluidic devices, including organ-on-chip models, contain bioengineered tissues or components of natural tissues or organs. These devices are designed to mimic the crucial structures and functions of living organisms.[111] The application of microfluidics in bioprinting makes it possible to create functional materials that include living cells. Microfluidic devices enable bioprinting with exceptionally precise control over small volumes ranging from 10^{-9} to 10^{-18} L of fluids.[112] This precision is achieved through carefully designed channels on the scale of tens of micrometers in diameter. The ability to control overflow, the capability, and the resolution to mix cells with bioinks in a controlled manner, make microfluidic systems an appealing tool for integration into bioprinting technology.[113] One application of microfluidic technology used in bioprinting is to develop microfluidic-based printheads to dispense multiple materials with high resolution.[114] One of the main challenges when using this technology is achieving control over the properties of the printed microtissue. CFD has been used to advance the convergence of microfluidic and bioprinting technologies. This integration aims to enhance the accuracy and control over achievable geometrical outcomes. **Figure 12** provides a comprehensive overview of the microfluidic printhead's schematic design and numerically modeled parameters. Each figure showcases the velocity, pressure, and shear rate fields within the microfluidic channels.[69]

3.4.5. Vascularization of Tissue Fabrication

The nature of tissue involves vascular structures that drive the perfusion of nutrients and oxygen to needy cells. Bioprinted cells struggle to survive for an extended period due to a lack of nutrients and oxygen or improper transfer of these essential elements to the cells. Vascularization poses a significant challenge in the field of bioprinting, and extensive research has been conducted to address this issue.[115] Successfully fabricating vascular tissue relies on achieving a balance between high resolution and a high throughput of perfusable channels within the printed construct. In this context, CFD plays a crucial role in aiding the fabrication of vascular structures within tissue by analyzing flow characteristics, including net force, pressure distribution, shear stress, and oxygen distribution, among others.[78,116] **Figure 13** provides an example of CFD application for vascularized tissue fabrication.[82] In the article, a custom-made self-supporting perfused (SSuPer) tissue construct model was analyzed using CFD (Ansys Fluent). Various analyses, including shear stress, pressure distribution, flow rate, and flow direction were conducted to support their experimental results. This highlights the potential of CFD in guiding the design process before the biofabrication of vascular tissue. Moreover, in another study, Figure 13a(i,ii) presents the results of shear stress analysis for the 81-channel design in both flow directions. Turbulent flow streamlines of shear stress are depicted in Figure 13(i) for forward and Figure 13(ii) for reverse directions at the inlet of the 16-channel construct, under a flow rate of 10 mL min^{-1} of cell culture media (α-MEM). Figure 13c illustrates the gauge pressure measured for all construct designs, fluids, flow rates, and directions. Constructs with blocked channels experienced upward forces in the forward flow direction, affecting construct stability.

4. Conclusion and Future Perspective

In the sectors of AM and tissue engineering, a recent positive amalgamation has come forth to address the challenges that traditional tissue engineering faces, such as irregular cell distribution on scaffolds, difficulty producing patient-specific tissues,

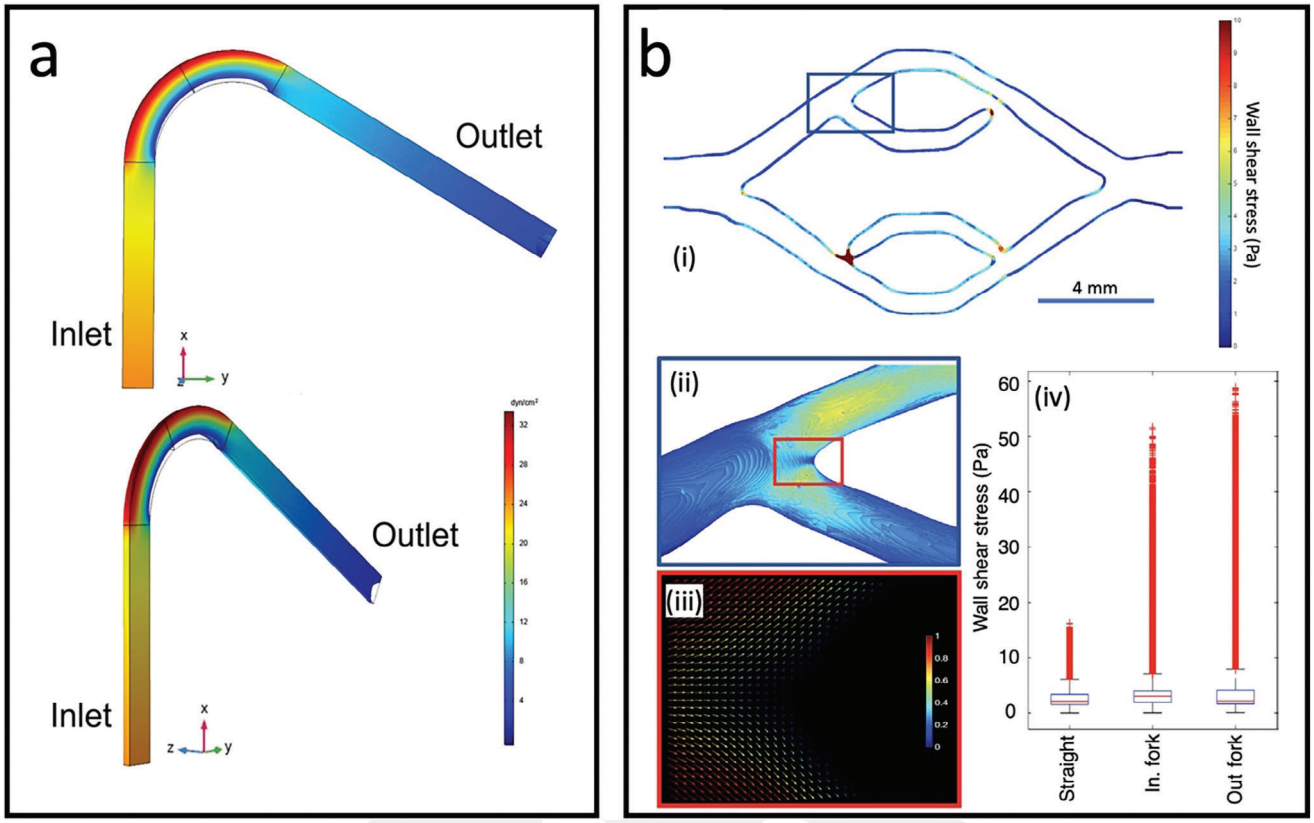

Figure 11. CFD for bioprinted blood vessels. a) The wall shear stresses (WSS) distribution in the vessel. Adapted with permission.[109] Copyright 2020, American Chemical Society. b) WSS and laminar flow dynamics during CTC perfusion. i) The WSS profile is shown from the vessel sidewalls at the center Z slice, derived from simulation data aligned with CTC perfusion experiment parameters. Seemingly disconnected channel branches result from Z height variation within the print, not actual breaks in the channels. ii) A closer view of the topmost vessel in-flow branching point, featuring the same heatmap as in (i), illustrates WSS at both the sidewalls and vessel floor. iii) A 2D quiver plot of the velocity field at the topmost branching point simulates the CTC perfusion experiment, demonstrating laminar, non-turbulent flow at a flow rate of 1690 µL min^{-1}. iv) A whisker plot compares WSS between straight vessels, in-flow branches, and out-flow branches within the endothelialized device. Reproduced with permission.[110] Copyright 2020, AAAS.

and limited cell density. Thus, the introduction of bioprinting has been monumental for tissue engineering by utilizing AM technologies to alleviate the aforementioned issues by constructing 3D cellular structures. These bioprinting processes, as mentioned in this review, are categorized into scaffold-based (extrusion, inkjet, and laser-based methods) and scaffold-free, as well as the more recent VBP methods. Moreover, CFD has emerged as indispensable in refining bioprinting processes. By simulating fluid flow, stress distribution, and other parameters, CFD minimizes the need for costly and time-consuming experimental iterations, optimizing factors such as bioink printability, cell viability, and nozzle design. This union between CFD and bioprinting has been critical in assessing the issues in tissue engineering due to the acceleration of the development of lab-grown tissues and organs. We have outlined the breakthroughs that have been attained due to researchers delving deeper into the complexities of fluid dynamics at the cellular level. Therefore, it can be said that the collaboration of CFD and tissue engineering has been an ongoing technological advancement, which inches us closer to a world where such engineered constructs would be the norm in the medical field for patients worldwide.

Moreover, VBP, also known as CAL, a relatively recent bioprinting technique, has been the highlight of bioprinting methods. CAL offers a departure from traditional layer-by-layer deposition methods by employing a photopolymerization process to create intricate 3D structures in a single step. VBP is a rapid and simultaneous fabrication compared to traditional layer-by-layer construction, where it has great scalability and efficiency for tissue engineering. However, there has been no research conducted on the CFD aspect of CAL to optimize bioink characteristics, which is an opening for further research. Therefore, the developing status of CAL has been a highlight, offering exciting prospects for accelerating the development of functional tissues and organs.

Furthermore, machine learning (ML) and artificial intelligence (AI) have been utilized in the CFD and tissue engineering sectors due to the increasing need for optimization and automation in different aspects of tissue engineering. As large amounts of data are assessed by ML algorithms, trends can be identified that can optimize bioprinting parameters, which would in turn reduce the cost of protracted preliminary test runs. The precision and efficiency of bioprinting methods can be improved as well due to the

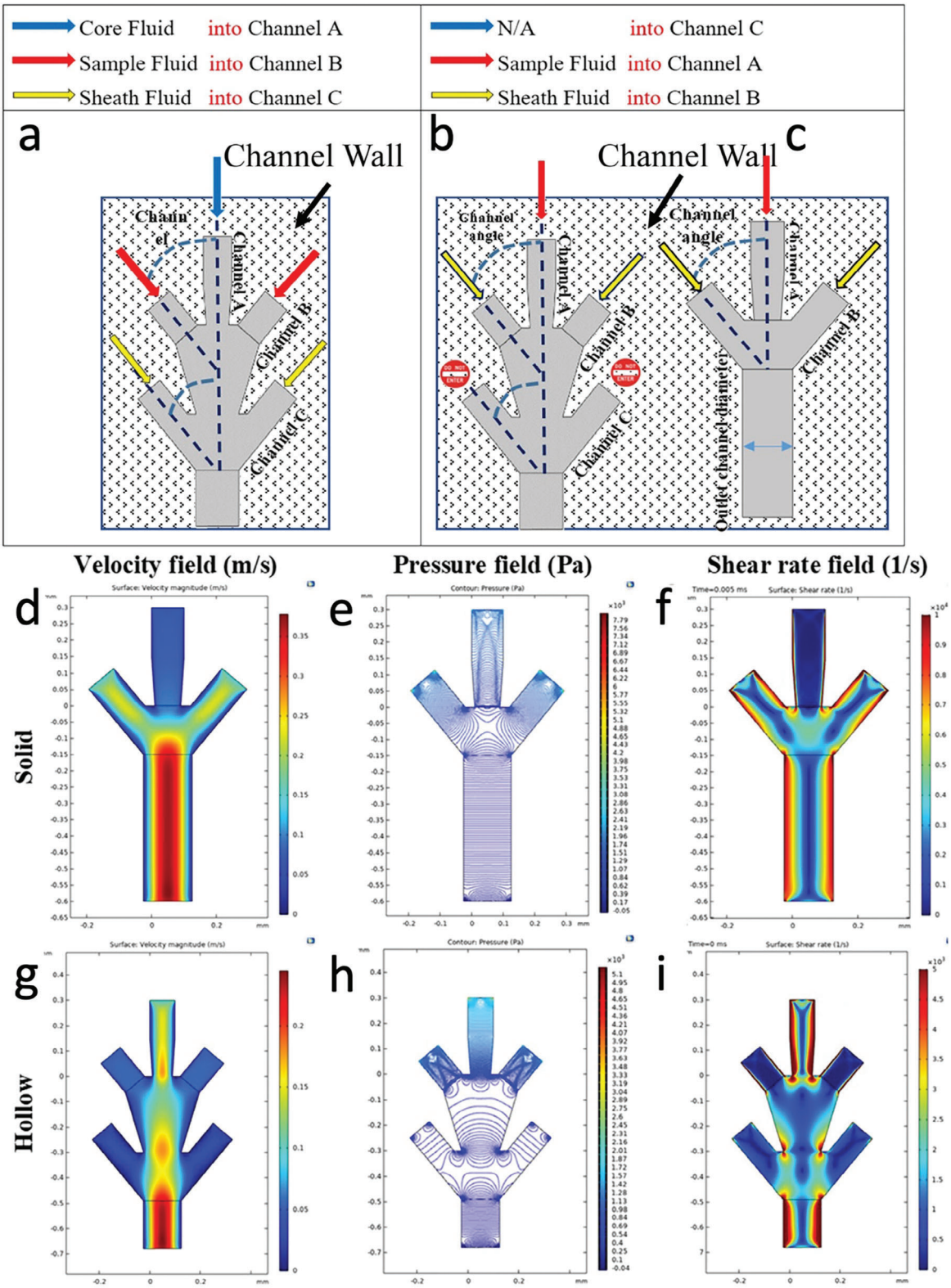

Figure 12. CFD analysis of microfluidic printhead. (a) depicts the schematic figure of the hollow microfiber fabrication system utilizing a microfluidic channel, while (b) illustrates the schematic figure of the solid microfiber fabrication system through the same microfluidic channel. d–i) Velocity field, pressure field, and shear rate field in the microfluidic channels embedded within the printhead system. d) Flow velocity field of solid microfiber, e) pressure field of solid microfiber, f) shear rate field of solid microfiber, g) flow velocity field of hollow microfiber, h) pressure field of hollow microfiber, i) shear rate field of hollow microfiber. Reproduced with permission.[69] Copyright 2022, Springer Nature.

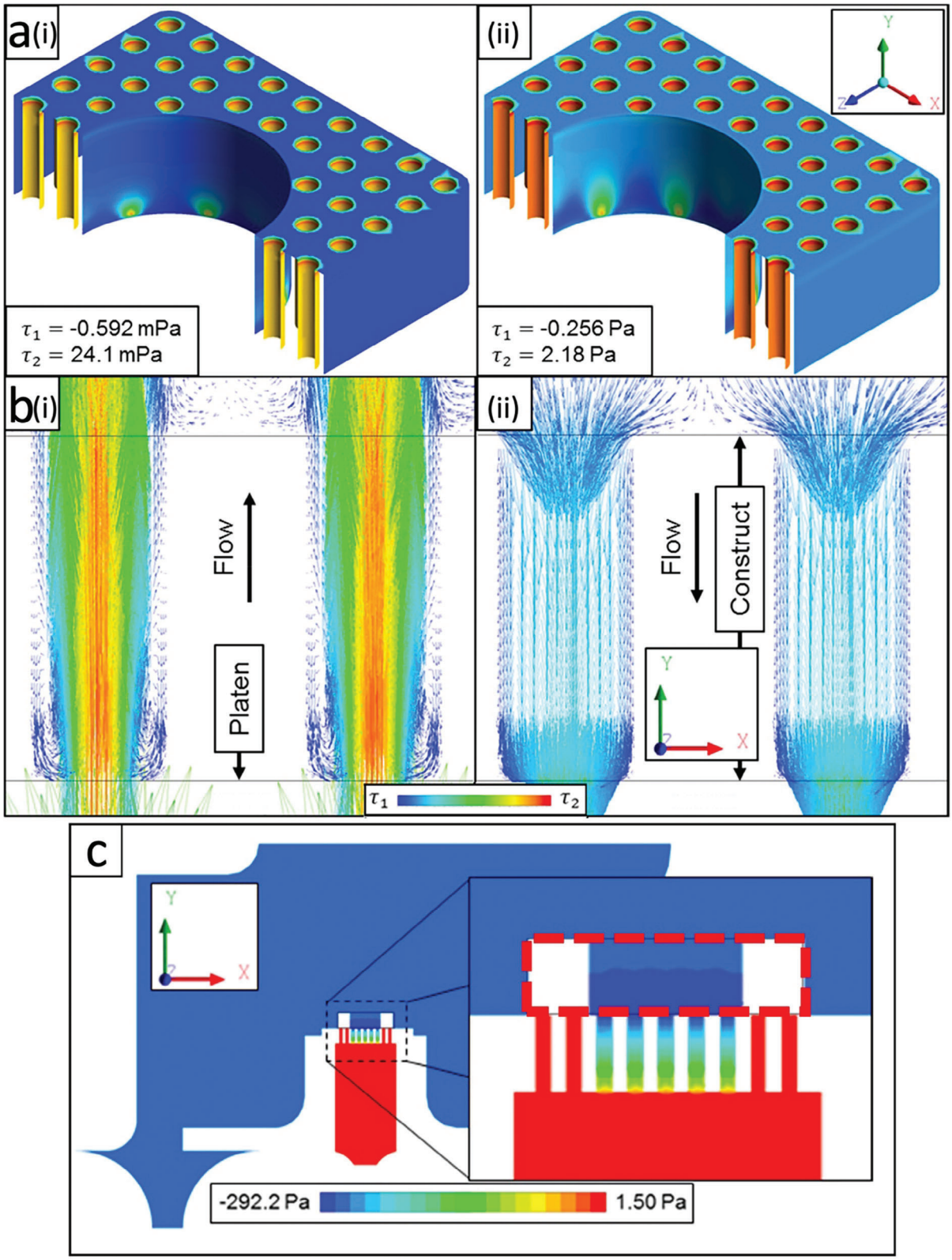

Figure 13. CFD application for vascular model involves multiple analyses. a) Shear stress on surfaces of the construct along the vertical direction for hybrid microchannel design perfused with a medium i) for 0.1 mL min^{-1} and ii) for 10 mL min^{-1}. b) Flow analysis of medium within the microchannel i) for forward and ii) for reverse directions. c) Pressure analysis in the *xy*–plane for single flow channel construct. Adapted with permission.[82] Copyright 2019, Wiley-VCH.

predictive modeling of AI, which can produce favorable results that are more precise and reproducible. Therefore, the incorporation of artificial intelligence into bioprinting can transform the tissue engineering industry, and thus, further development in regenerative medicine and paving the road for personalized healthcare solutions can be done.

Acknowledgements

The authors would like to acknowledge Abdullah Gul University for giving an opportunity to work together.

Conflict of Interest

The authors declare no conflict of interest.

Keywords

bioprinter, bioprinting, computational fluid dynamics analysis, computation fluid dynamics (CFD), types of bioprinting

Received: February 20, 2024
Revised: April 14, 2024
Published online: May 2, 2024

[1] A. DC, R. D, R. M, L. PVS, M. A, D. G, *J. Mech. Behav. Biomed. Mater.* **2017**, *69*, 401.
[2] V. S, Y. WC, L. WF, W. CH, F. JYH, *Adv. Drug Delivery Rev.* **2018**, *132*, 296.
[3] J. P. Vacanti, R. Langer, *Lancet* **1999**, *354*, S32.
[4] C. A. Vacanti, *J. Cell. Mol. Med.* **2006**, *10*, 569.
[5] D. A. S. Rodríguez, A. I. Ramos-Murillo, R. D. Godoy-Silva, *Int. J. Bioprint.* **2021**, *24*, e00171.
[6] C.-C. Pan, A. Bruyas, Y. P. Yang, *Mater. Matters* **2016**, *11*, 49.
[7] M. L, B. T, B. JA, D. M. C, D. B, F. G, G. J, L. Q, M. J, M. VA, M. C, N. M, S. W, T. S, W. TBF, X. T, Y. JJ, V. G., *Trends Biotechnol.* **2018**, *36*, 384.
[8] N. P. Bernal, P. Delrot, D. Loterie, Y. Li, J. Malda, C. Moser, R. Levato, *Adv. Mater.* **2019**, *31*, 1904209.
[9] E. I. Basri, A. A. Basri, V. N. Riazuddin, S. F. Shahwir, Z. Mohammad, K. A. Ahmad, *Int. J. Fluids Heat Transfer* **2016**, *1*, 2.
[10] P. R. Spalart, V. Venkatakrishnan, *J. Aeronaut. Sci.* **2016**, *120*, 209.
[11] O. J. Boelens, *Aerosp. Sci. Technol.* **2012**, *20*, 38.
[12] R. Chand, B. S. Muhire, S. Vijayavenkataraman, *Int. J. Bioprint.* **2022**, *8*, 545.
[13] J. Leppiniemi, P. Lahtinen, A. Paajanen, R. Mahlberg, S. Metsä-Kortelainen, T. Pinomaa, H. Pajari, I. Vikholm-Lundin, P. Pursula, V. P. Hytönen, *ACS Appl. Mater. Interfaces* **2017**, *9*, 21959.
[14] A. Malekpour, X. Chen, *J. Funct. Biomater.* **2022**, *13*, 40.
[15] I. O. Smith, X. H. Liu, L. A. Smith, P. X. Ma, *Wiley Interdiscip. Rev.: Nanomed. Nanobiotechnol.* **2009**, *1*, 226.
[16] A. B. Dababneh, I. T. Ozbolat, *J. Manuf. Sci. Eng.* **2014**, *136*, 061016.
[17] R. J. Klebe, *Exp. Cell Res.* **1988**, *179*, 362.
[18] I. T. Ozbolat, *Trends Biotechnol.* **2015**, *33*, 395.
[19] P. Datta, A. Barui, Y. Wu, V. Ozbolat, K. K. Moncal, I. T. Ozbolat, *Biotechnol. Adv.* **2018**, *36*, 1481.
[20] J. Zhang, E. Wehrle, M. Rubert, R. Müller, *Int. J. Mol. Sci.* **2021**, *22*, 3971.
[21] S. Knowlton, S. Onal, C. H. Yu, J. J. Zhao, S. Tasoglu, *Trends Biotechnol.* **2015**, *33*, 504.
[22] E. Lepowsky, M. Muradoglu, S. Tasoglu, *Int. J. Bioprint.* **2018**, *11*, e00034.
[23] I. T. Ozbolat, M. Hospodiuk, *Biomaterials* **2016**, *76*, 321.
[24] S. V. Murphy, A. Atala, *Nat. Biotechnol.* **2014**, *32*, 773.
[25] B. Yenilmez, M. Temirel, S. Knowlton, E. Lepowsky, S. Tasoglu, *Int. J. Bioprint.* **2019**, *13*, e00044.
[26] S. Khalil, J. Nam, W. Sun, *Rapid Prototyping J.* **2005**, *11*, 9.
[27] A. Skardal, J. Zhang, L. McCoard, X. Xu, S. Oottamasathien, G. D. Prestwich, *Tissue Eng., Part A* **2010**, *16*, 2675.
[28] H. Gudapati, M. Dey, I. Ozbolat, *Biomaterials* **2016**, *102*, 20.
[29] T. Goldmann, J. S. Gonzalez, *J. Biochem. Biophys. Methods* **2000**, *42*, 105.
[30] E. Tekin, P. J. Smith, U. S. Schubert, *Soft Matter* **2008**, *4*, 703.
[31] F. Guillemot, B. Guillotin, A. Fontaine, M. Ali, S. Catros, V. Kériquel, J.-C. Fricain, M. Rémy, R. Bareille, J. Amédée-Vilamitjana, *MRS Bull.* **2011**, *36*, 1015.
[32] a) M. T. Sultan, O. J. Lee, J. S. Lee, C. H. Park, *Biomedicines* **2022**, *10*, 3224; b) W. Li, M. Wang, H. Ma, F. A. Chapa-Villarreal, A. O. Lobo, Y. S. Zhang, *iScience* **2023**, *26*, 106039.
[33] a) J. Zhang, Q. Hu, S. Wang, J. Tao, M. Gou, *Int. J. Bioprint.* **2020**, *6*, 242; b) L. Y, M. G, S. G, C. S, R. K, *J. Biomed. Mater. Res., Part A* **2006**, *77*, 396.
[34] a) X. Jing, H. Fu, B. Yu, M. Sun, L. Wang, *Front. Bioeng. Biotechnol.* **2022**, *10*, 994355; b) G. Weisgrab, O. Guillaume, Z. Guo, P. Heimel, P. Slezak, A. Poot, D. Grijpma, A. Ovsianikov, *Biofabrication* **2020**, *12*, 045036.
[35] A. Alghuwainem, A. T. Alshareeda, B. Alsowayan, *Int. J. Mol. Sci.* **2019**, *20*, 4926.
[36] N. I. Moldovan, *J. Cell. Mol. Med.* **2018**, *22*, 2964.
[37] B. Kelly, I. Bhattacharya, M. Shusteff, R. M. Panas, H. K. Taylor, C. M. Spadaccini, arXiv preprint arXiv:1705.05893, **2017**.
[38] Z. T, F. S, L. R, O. A, *Trends Biotechnol.* **2023**, *41*, 604.
[39] D. Ribezzi, M. Gueye, S. Florczak, F. Dusi, D. de Vos, F. Manente, A. Hierholzer, M. Fussenegger, M. Caiazzo, T. Blunk, J. Malda, R. Levato, *Adv. Mater.* **2023**, *35*, 2301673.
[40] a) L. Lian, M. Xie, Z. Luo, Z. Zhang, S. Maharjan, X. Mu, C. E. Garciamendez-Mijares, X. Kuang, J. K. Sahoo, G. Tang, G. Li, D. Wang, J. Guo, F. Z. Gonzalez, V. Abril Manjarrez Rivera, L. Cai, X. Mei, D. L. Kaplan, Y. S. Zhang, *Adv. Mater.* **2024**, 2304846; b) S. Jing, L. Lian, Y. Hou, Z. Li, Z. Zheng, G. Li, G. Tang, G. Xie, M. Xie, *Biofabrication* **2023**, *16*, 012004; c) M. Xie, L. Lian, X. Mu, Z. Luo, C. E. Garciamendez-Mijares, Z. Zhang, A. López, J. Manríquez, X. Kuang, J. Wu, J. K. Sahoo, F. Z. González, G. Li, G. Tang, S. Maharjan, J. Guo, D. L. Kaplan, Y. S. Zhang, *Nat. Commun.* **2023**, *14*, 210.
[41] U. Jammalamadaka, K. Tappa, *J. Funct. Biomater.* **2018**, *9*, 22.
[42] R. B. Heimann, *Materials for Medical Application*, Walter de Gruyter, Berlin **2020**.
[43] J. Shin, Y. Lee, Z. Li, J. Hu, S. S. Park, K. Kim, *Micromachines* **2022**, *13*, 363.
[44] E. T. Jiann Chong, J. W. Ng, P.-C. Lee, *BIO Integr.* **2022**, *4*, 54.
[45] A. B. Balaji, H. Pakalapati, M. Khalid, R. Walvekar, H. Siddiqui, *Biodegrad. Biocompat. Polym. Compos.* **2018**, *286*, 3.
[46] S. F. Badylak, *Naturally Occurring Scaffold Materials*, Elsevier, Amsterdam **2010**.
[47] J. Groll, J. A. Burdick, D.-W. Cho, B. Derby, M. Gelinsky, S. C. Heilshorn, T. Juengst, J. Malda, V. A. Mironov, K. Nakayama, *Biofabrication* **2018**, *11*, 013001.
[48] A. L. Rutz, K. E. Hyland, A. E. Jakus, W. R. Burghardt, R. N. Shah, *Adv. Mater.* **2015**, *27*, 1607.
[49] M. Hospodiuk, M. Dey, D. Sosnoski, I. T. Ozbolat, *Biotechnol. Adv.* **2017**, *35*, 217.

[50] I. T. Ozbolat, *3D Bioprinting: Fundamentals, Principles and Applications*, Academic Press, Cambridge, MA **2016**.
[51] D. Murata, K. Arai, K. Nakayama, *Adv. Healthcare Mater.* **2020**, *9*, 1901831.
[52] R. R. Jose, M. J. Rodriguez, T. A. Dixon, F. Omenetto, D. L. Kaplan, *ACS Biomater. Sci. Eng.* **2016**, *2*, 1662.
[53] J. Maitra, V. K. Shukla, *Am. J. Polym. Sci.* **2014**, *4*, 25.
[54] A. GhavamiNejad, N. Ashammakhi, X. Y. Wu, A. Khademhosseini, *Small* **2020**, *16*, 2002931.
[55] L. Voorhaar, R. Hoogenboom, *Chem. Soc. Rev.* **2016**, *45*, 4013.
[56] a) J. Berger, M. Reist, J. M. Mayer, O. Felt, N. A. Peppas, R. Gurny, *Eur. J. Pharm. Biopharm.* **2004**, *57*, 19; b) C. K. Kuo, P. X. Ma, *Biomaterials* **2001**, *22*, 511.
[57] a) S. L. Bourke, M. Al-Khalili, T. Briggs, B. B. Michniak, J. Kohn, L. A. Poole-Warren, *AAPS PharmSci* **2003**, *5*, 101; b) I. Mironi-Harpaz, D. Y. Wang, S. Venkatraman, D. Seliktar, *Acta Biomater.* **2012**, *8*, 1838.
[58] S. Kobayashi, H. Uyama, S. Kimura, *Chem. Rev.* **2001**, *101*, 3793.
[59] W. Hu, Z. Wang, Y. Xiao, S. Zhang, J. Wang, *Biomater. Sci.* **2019**, *7*, 843.
[60] M. Kawaguti, *J. Phys. Soc. Jpn.* **1953**, *8*, 747.
[61] L. F. Richardson, *Weather Prediction by Numerical Process*, Cambridge University Press, Cambridge **2007**.
[62] K. Z. K. Shaari, M. Awang, *Engineering Applications of Computational Fluid Dynamics*, Springer, Berlin **2015**.
[63] J. Göhl, K. Markstedt, A. Mark, K. Håkansson, P. Gatenholm, F. Edelvik, *Biofabrication* **2018**, *10*, 034105.
[64] J. W Jung, H.-G. Yi, T.-Y. Kang, W.-J. Yong, S. Jin, W.-S. Yun, D.-W. Cho, *J. Biomech. Eng.* **2013**, *135*, 84501.
[65] I. P. Magalhães, P. M. d. Oliveira, J. Dernowsek, E. B. L. Casas, M. S. L. Casas, *Matéria* **2019**, *24*, e12401.
[66] a) G. Gillispie, P. Prim, J. Copus, J. Fisher, A. G. Mikos, J. J. Yoo, A. Atala, S. J. Lee, *Biofabrication* **2020**, *12*, 022003; b) S. Naghieh, X. Chen, *J. Pharm. Anal.* **2021**, *11*, 564.
[67] J. Hendriks, C. Willem Visser, S. Henke, J. Leijten, D. B. F. Saris, C. Sun, D. Lohse, M. Karperien, *Sci. Rep.* **2015**, *5*, 11304.
[68] E. Reina-Romo, S. Mandal, P. Amorim, V. Bloemen, E. Ferraris, L. Geris, *Front. Bioeng. Biotechnol.* **2021**, *9*.
[69] A. Zaeri, R. Zgeib, K. Cao, F. Zhang, R. C. Chang, *Sci. Rep.* **2022**, *12*, 3364.
[70] M. Müller, E. Öztürk, Ø. Arlov, P. Gatenholm, M. Zenobi-Wong, *Ann. Biomed. Eng.* **2017**, *45*, 210.
[71] L. Ning, N. Betancourt, D. J. Schreyer, X. Chen, *ACS Biomater. Sci. Eng.* **2018**, *4*, 3906.
[72] T. Billiet, E. Gevaert, T. De Schryver, M. Cornelissen, P. Dubruel, *Biomaterials* **2014**, *35*, 49.
[73] A. Bahrd, Computational Fluid Dynamics and Quantitative Cell Viability Measurements in Dispensing-Based Biofabrication, Master thesis, Umea University, **2017**.
[74] M. Steuperaert, C. Debbaut, C. Carlier, O. De Wever, B. Descamps, C. Vanhove, W. Ceelen, P. Segers, *Drug Delivery* **2019**, *26*, 404.
[75] C.-T. Kuo, C.-L. Chiang, C.-H. Chang, H.-K. Liu, G.-S. Huang, R. Y.-J. Huang, H. Lee, C.-S. Huang, A. M. Wo, *Biomaterials* **2014**, *35*, 1562.
[76] V. S. Shirure, Y. Bi, M. B. Curtis, A. Lezia, M. M. Goedegebuure, S. P. Goedegebuure, R. Aft, R. C. Fields, S. C. George, *Lab Chip* **2018**, *18*, 3687.
[77] a) W. Liu, M. A. Heinrich, Y. Zhou, A. Akpek, N. Hu, X. Liu, X. Guan, Z. Zhong, X. Jin, A. Khademhosseini, Y. S. Zhang, *Adv. Healthcare Mater.* **2017**, *6*, 1601451; b) L. Lemarié, A. Anandan, E. Petiot, C. Marquette, E.-J. Courtial, *Int. J. Bioprint.* **2021**, *21*, e00119.
[78] M. L. Tomov, L. Perez, L. Ning, H. Chen, B. Jing, A. Mingee, S. Ibrahim, A. S. Theus, G. Kabboul, K. Do, S. R. Bhamidipati, J. Fischbach, K. McCoy, B. A. Zambrano, J. Zhang, R. Avazmohammadi, A. Mantalaris, B. D. Lindsey, D. Frakes, H. Bauser-Heaton, *Adv. Healthcare Mater.* **2021**, *10*, 2100968.
[79] J. Emmermacher, D. Spura, J. Cziommer, D. Kilian, T. Wollborn, U. Fritsching, J. Steingroewer, T. Walther, M. Gelinsky, A. Lode, *Biofabrication* **2020**, *12*, 025022.
[80] J. Shi, B. Wu, S. Li, J. Song, B. Song, W. F. Lu, *Biomed. Phys. Eng. Exp.* **2018**, *4*, 045028.
[81] Y. Yao, W. D. Chen, W. Y. Jin, *Adv. Mater. Res.* **2011**, *308*, 771.
[82] T. J. Sego, M. Prideaux, J. Sterner, B. P. McCarthy, P. Li, L. F. Bonewald, B. Ekser, A. Tovar, L. Jeshua Smith, *Biotechnol. Bioeng.* **2020**, *117*, 798.
[83] M. L. Tomov, A. Cetnar, K. Do, H. Bauser-Heaton, V. Serpooshan, *J. Am. Heart Assoc.* **2019**, *8*, e014490.
[84] J. Qu, C. Dou, B. Xu, J. Li, Z. Rao, A. Tsin, *arXiv:2103.09125* **2021**.
[85] J. Brindha, R. A. G. Privita Edwina, P. K. Rajesh, P. Rani, *Mater. Today* **2016**, *3*, 3285.
[86] L. M. Friedrich, R. T. Gunther, J. E. Seppala, *Phys. Fluids* **2022**, *34*, 083112.
[87] K. Hölzl, S. Lin, L. Tytgat, S. Van Vlierberghe, L. Gu, A. Ovsianikov, *Biofabrication* **2016**, *8*, 032002.
[88] C. W. Visser, P. E. Frommhold, S. Wildeman, R. Mettin, D. Lohse, C. Sun, *Soft Matter* **2015**, *11*, 1708.
[89] P. Behrouzi, M. Zali, M. Muhaddesi, A. Hashemi, A. Khoradmehr, A. T. Jahromi, I. Nabipour, A. Tamadon, *Res Sq* **2021**, https://doi.org/10.21203/rs.3.rs-181593/v1
[90] N. Hasan, Y. B. Mathur, *International Multidisciplinary Mulitilingual E-Journal*, *5*, 19.
[91] H. K. Versteeg, W. Malalasekera, *An Introduction to Computational Fluid Dynamics: The Finite Volume Method*, 2nd ed., Pearson, London **2007**.
[92] S. Zhang, S. Vijayavenkataraman, W. F. Lu, J. Y. H. Fuh, *J. Biomed. Mater. Res., Part B* **2019**, *107*, 1329.
[93] P. Wang, Y. Sun, L. Diao, H. Liu, *Int. J. Bioprint.* **2024**, 2362.
[94] C. F. Ceballos-González, E. J. Bolívar-Monsalve, D. A. Quevedo-Moreno, C. Chávez-Madero, S. Velásquez-Marín, L. L. Lam-Aguilar, Ó. E. Solís-Pérez, A. Cantoral-Sánchez, M. Neher, E. Yzar-García, *Adv. Mater. Technol.* **2023**, *8*, 2202208.
[95] K. Song, D. Zhang, J. Yin, Y. Huang, *Addit. Manuf.* **2021**, *41*, 101963.
[96] M. Nooranidoost, D. Izbassarov, S. Tasoglu, M. Muradoglu, *Phys. Fluids* **2019**, *31*, 081901.
[97] A. D. Cetnar, M. L. Tomov, L. Ning, B. Jing, A. S. Theus, A. Kumar, A. N. Wijntjes, S. R. Bhamidipati, K. P. Do, A. Mantalaris, J. N. Oshinski, R. Avazmohammadi, B. D. Lindsey, H. D. Bauser-Heaton, V. Serpooshan, *Adv. Healthcare Mater.* **2021**, *10*, e2001169.
[98] H. J. McLennan, A. J. Blanch, S. J. Wallace, L. J. Ritter, S. L. Heinrich, D. K. Gardner, K. R. Dunning, M. J. Gauvin, A. K. Love, J. G. Thompson, *Sci. Rep.* **2023**, *13*, 562.
[99] P. Kumar, S. Ebbens, X. Zhao, *Int. J. Bioprint.* **2021**, *23*, e00157.
[100] Z. Zhang, Y. Jin, J. Yin, C. Xu, R. Xiong, K. Christensen, B. R. Ringeisen, D. B. Chrisey, Y. Huang, *Appl. Phys. Rev.* **2018**, *5*, 041304.
[101] a) N. Soltan, L. Ning, F. Mohabatpour, P. Papagerakis, X. Chen, *ACS Biomater. Sci. Eng.* **2019**, *5*, 2976; b) M. D. Sarker, S. Naghieh, A. D. McInnes, L. Ning, D. J. Schreyer, X. Chen, *Int. J. Bioprint.* **2019**, *14*, e00045.
[102] G. Ates, P. Bartolo, *Int. J. Bioprint.* **2023**, *9*, 0219.
[103] J. Adhikari, A. Roy, A. Das, M. Ghosh, S. Thomas, A. Sinha, J. Kim, P. Saha, *Macromol. Biosci.* **2021**, *21*, 2000179.
[104] a) S. Boularaoui, G. Al Hussein, K. A. Khan, N. Christoforou, C. Stefanini, *Int. J. Bioprint.* **2020**, *20*, e00093; b) A. Blaeser, D. F. Duarte Campos, U. Puster, W. Richtering, M. M. Stevens, H. Fischer, *Adv. Healthcare Mater.* **2016**, *5*, 326; c) J. C. Gomez-Blanco, J. B. Pagador, V. P. Galvan-Chacon, L. F. Sanchez-Peralta, M. Matamoros, A. Marcos, F. M. Sanchez-Margallo, *Int. J. Bioprint.* **2023**, *9*, 730.
[105] a) N. Paxton, W. Smolan, T. Böck, F. Melchels, J. Groll, T. Jungst, *Biofabrication* **2017**, *9*, 044107; b) R. Sharma, I. P. M. Smits, L. De La

Vega, C. Lee, S. M. Willerth, *Front. Bioeng. Biotechnol.* **2020**, *8*, 57; c) J. M. Lee, W. Y. Yeong, *Virtual Phys. Prototyping* **2015**, *10*, 3.
[106] T. Stolarski, Y. Nakasone, S. Yoshimoto, *Engineering Analysis with ANSYS Software*, Butterworth-Heinemann, Oxford **2018**.
[107] J. Choi, E. J. Lee, W. B. Jang, S.-M. Kwon, *J. Funct. Biomater.* **2023**, *14*, 497.
[108] W. Park, J. S. Lee, G. Gao, B. S. Kim, D. W. Cho, *Nat. Commun.* **2023**, *14*, 7696.
[109] X. Zhou, M. Nowicki, H. Sun, S. Y. Hann, H. Cui, T. Esworthy, J. D. Lee, M. Plesniak, L. G. Zhang, *ACS Appl. Mater. Interfaces* **2020**, *12*, 45904.
[110] W. F. Hynes, M. Pepona, C. Robertson, J. Alvarado, K. Dubbin, M. Triplett, J. J. Adorno, A. Randles, M. L. Moya, *Sci. Adv.* **2020**, *6*, eabb3308.
[111] M. A. Chliara, S. Elezoglou, I. Zergioti, *Biosensors* **2022**, *12*, 1135.
[112] E. Davoodi, E. Sarikhani, H. Montazerian, S. Ahadian, M. Costantini, W. Swieszkowski, S. M. Willerth, K. Walus, M. Mofidfar, E. Toyserkani, *Adv. Mater. Technol.* **2020**, *5*, 1901044.
[113] a) G. M. Whitesides, *Nature* **2006**, *442*, 368; b) A. K. Miri, E. Mostafavi, D. Khorsandi, S.-K. Hu, M. Malpica, A. Khademhosseini, *Biofabrication* **2019**, *11*, 042002.
[114] a) Y. Yu, W. Wei, Y. Wang, C. Xu, Y. Guo, J. Qin, *Adv. Mater.* **2016**, *28*, 6649; b) E. Kang, G. S. Jeong, Y. Y. Choi, K. H. Lee, A. Khademhosseini, S.-H. Lee, *Nat. Mater.* **2011**, *10*, 877.
[115] a) P. Datta, B. Ayan, I. T. Ozbolat, *Acta Biomater.* **2017**, *51*, 1; b) D. Richards, J. Jia, M. Yost, R. Markwald, Y. Mei, *Ann. Biomed. Eng.* **2017**, *45*, 132; c) Z. A. Sexton, A. R. Hudson, J. E. Herrmann, D. J. Shiwarski, J. Pham, J. M. Szafron, S. M. Wu, M. Skylar-Scott, A. W. Feinberg, A. Marsden, *arXiv:2308.07586* **2023**.
[116] L. Pourchet, E. Petiot, C. Loubière, E. Olmos, M. Dos Santos, A. Thépot, B. J. Loïc, C. A. Marquette, *Int. J. Bioprint.* **2019**, *13*, e00039.

Umar Naseef received his B.S. degree in Mechanical Engineering from Abdullah Gül University in 2023. Currently, he works as a mechanical engineer in Saudi Arabia and pursues independent research endeavors. His research interests span two focal areas: the application of CFD for bioprinting and fiber-reinforced composite materials.

Syed Ali Arsal Naqvi received his bachelor's degree from Abdullah Gül University in 2023 with high honors. Currently, he works as a mechanical engineer in Turkey and is doing independent research. His current research focuses on the application of CFD in analyzing and optimizing various bioprinting nozzle types for increased cell viability.

Makame Mahmud received his bachelor's degree from Abdullah Gül University in 2024 with honors. Currently, he works as a mechanical engineer in Turkey. Along with this, he is doing independent research. His research focuses on 3D printing, CFD for bioprinting, and metal 3D printing.

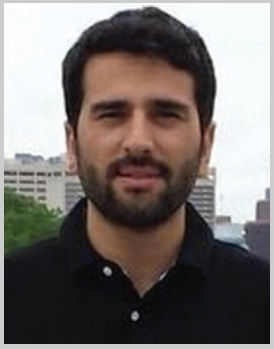

Mikail Temirel received his master's degree in Mechanical Engineering in 2015 and his Ph.D. in Biomedical Engineering in 2021 from Drexel University and the University of Connecticut in the USA, respectively. He joined the Mechanical Engineering Department at Abdullah Gul University in Turkey as an assistant professor in 2021. His current research focuses on bioprinting, point-of-care devices, and paper and fabric-based microfluidics devices.